Deformation in the Stensgar Mountain Quadrangle, Stevens County, Washington

U.S. GEOLOGICAL SURVEY BULLETIN 1820

Deformation in the Stensgar Mountain Quadrangle, Stevens County, Washington

By JAMES G. EVANS

U.S. GEOLOGICAL SURVEY BULLETIN 1820

DEPARTMENT OF THE INTERIOR
DONALD PAUL HODEL, Secretary

U.S. GEOLOGICAL SURVEY
Dallas L. Peck, Director

UNITED STATES GOVERNMENT PRINTING OFFICE, WASHINGTON : 1988

For sale by the
Books and Open-File Reports Section
U.S. Geological Survey
Federal Center, Box 25425
Denver, CO 80225

Library of Congress Cataloging-in-Publication Data

Evans, James George, 1938–
Deformation in the Stensgar Mountain quadrangle, Stevens County, Washington.

(U.S. Geological Survey Bulletin ; 1820)
Bibliography: p.
Supt. of Docs. no. : I 19.3:1820
1. Rock deformation—Washington (state)—Stevens County. 2. Geology, Structural. 3. Geology—Washington (State)—Stevens County. I. Title.
II. Series.
QE75.B9 no. 1820 557.3 s 88-600279
[QE604] [551.8'09797'23]

CONTENTS

PLATE
[In pocket]

FIGURES

TABLE

Deformation in the Stensgar Mountain Quadrangle, Stevens County, Washington

By James G. Evans

Abstract

Most deformation of the Middle and Late Proterozoic (Deer Trail and Windermere Groups) and Lower Cambrian (Addy Quartzite and Old Dominion Limestone) rocks in the Stensgar Mountain quadrangle occurred during the Mesozoic (pre-Late Jurassic, possibly Early Jurassic or Triassic), in connection with duplex thrusting. The principal deformation occurred in stages that generally involved: (1) thrusting, (2) penetrative dynamothermal metamorphism in the greenschist facies, and (3) renewed thrusting. The initial thrusting may have included formation of the duplex fault zone, moderate tilting of the sedimentary and volcanic rocks, and possibly low-grade metamorphism. The dynamothermal metamorphism resulted in development of a slaty cleavage that dips steeply west, as well as numerous minor and a few large folds that plunge at low to moderate angles, generally north. The folds have axial planes parallel to cleavage. Clasts in conglomerates were flattened parallel to cleavage, and their long axes were aligned north-northeastward, subparallel to fold axes. This extension direction parallels the trend of the Kootenay arc, a relation not typical of orogenic belts. The dynamothermal metamorphism included coaxial compressive pulses separated by periods of stress relaxation. The penetrative deformation could have been accompanied by slip on preexisting faults, including a large strike-slip component for the roof (Stensgar Mountain thrust) and floor (Lane Mountain thrust) thrusts of the duplex fault zone. Later movements along these roof and floor thrusts and connecting splays are suggested by nonfolded traces of the faults and the faulted, dynamothermally metamorphosed cataclasite adjacent to the Lane Mountain thrust.

The penetrative deformation that affected the Stensgar Mountain quadrangle also affected the rest of northeastern Washington and southeastern British Columbia; it may have been the result of oblique convergence during Mesozoic subduction.

INTRODUCTION

The Stensgar Mountain $7^1/_2$-minute quadrangle, located 12 km southwest of Chewelah, Stevens County, northeastern Washington, is underlain by an 8-km-thick section consisting of the Proterozoic Deer Trail and Windermere Groups, and the Cambrian Addy Quartzite and Old Dominion Limestone (fig. 1). The study area includes part of the "magnesite belt" (Bennett, 1941, p. 3), a term used to refer to the zone of crystalline magnesite deposits that occur in the Stensgar Dolomite, one of the formations in the Deer Trail Group. As used by Campbell and Loofbourow (1962, p. F2), this term also includes formations adjacent to the dolomite. The magnesite belt lies along the Kootenay arc (Hedley, 1955; White, 1959; Fyles, 1962; Yates and others, 1966; Yates, 1970), a narrow, arcuate belt of folded and faulted rocks in northeastern Washington and adjacent British Columbia. The relation of the Deer Trail Group to the nearby, more widespread and widely known Proterozoic Belt Supergroup is not clearly understood. The Deer Trail Group may be correlative with the upper part of the Belt Supergroup, but unit-by-unit correlations have not yet been agreed upon (see discussion in Evans, 1987). Differences between the Deer Trail Group and the adjacent part of the Belt Supergroup in the Chewelah-Loon Lake area include possible facies changes between the two assemblages and greater intensity of deformation in the Deer Trail Group (Evans, 1987). The Deer Trail Group is complexly faulted and weakly metamorphosed.

This report describes minor structures in the Deer Trail Group and in later Proterozoic and Paleozoic rocks in the Stensgar Mountain quadrangle. Certain aspects of the deformation in this segment of the magnesite belt are characterized: the type and orientations of structures, degree of homogeneity of the deformation, strain history, and the relation of local deformation to regional events affecting the Kootenay arc.

GEOLOGY

The Stensgar Mountain quadrangle contains a section of the Middle Proterozoic Deer Trail Group at least 4,000 m thick, a section of the Middle(?) and Late Proterozoic Windermere Group possibly at least 1,700 m thick, and a section of Lower Cambrian strata at least 2,600 m thick (fig. 2). The Deer Trail Group consists of the following units, from oldest to youngest: the Togo Formation (slate, siltite, quartzite), the Edna Dolomite, the McHale Slate, the Stensgar Dolomite, and the Buffalo Hump Formation (slate, quartzite, and conglomerate). These formational names are adopted from the magnesite-belt nomenclature of Campbell and Loofbourow (1962). The Windermere

Publication authorized by the Director, U.S. Geological Survey, September 16, 1987.

Group comprises the Huckleberry Formation (basal conglomerate member and upper member of metabasalt and metatuff) and the Monk Formation (slate, conglomerate, and dolomite). Gabbro and metabasalt feeder dikes of metabasalt flows of the Huckleberry Formation intruded the Deer Trail Group and conglomerate of the Huckleberry Formation, causing minor contact metamorphism. The Lower Cambrian Addy Quartzite (1,100 m thick) was deposited unconformably on the Proterozoic rocks and subsequently covered by a thick section of the Old Dominion Limestone, only 1,500 m of which is within the study area. These rocks were described in detail by Evans (1987). Previous interpretations of the structure of the magnesite belt, including the Stensgar Mountain area, viewed the major structure as the western limb of a tightly folded and locally overturned anticline trending north-northeast (Weaver, 1920, p. 108; Bennett, 1941, p. 10; Campbell and Loofbourow, 1962, p. F32). The hinge zone

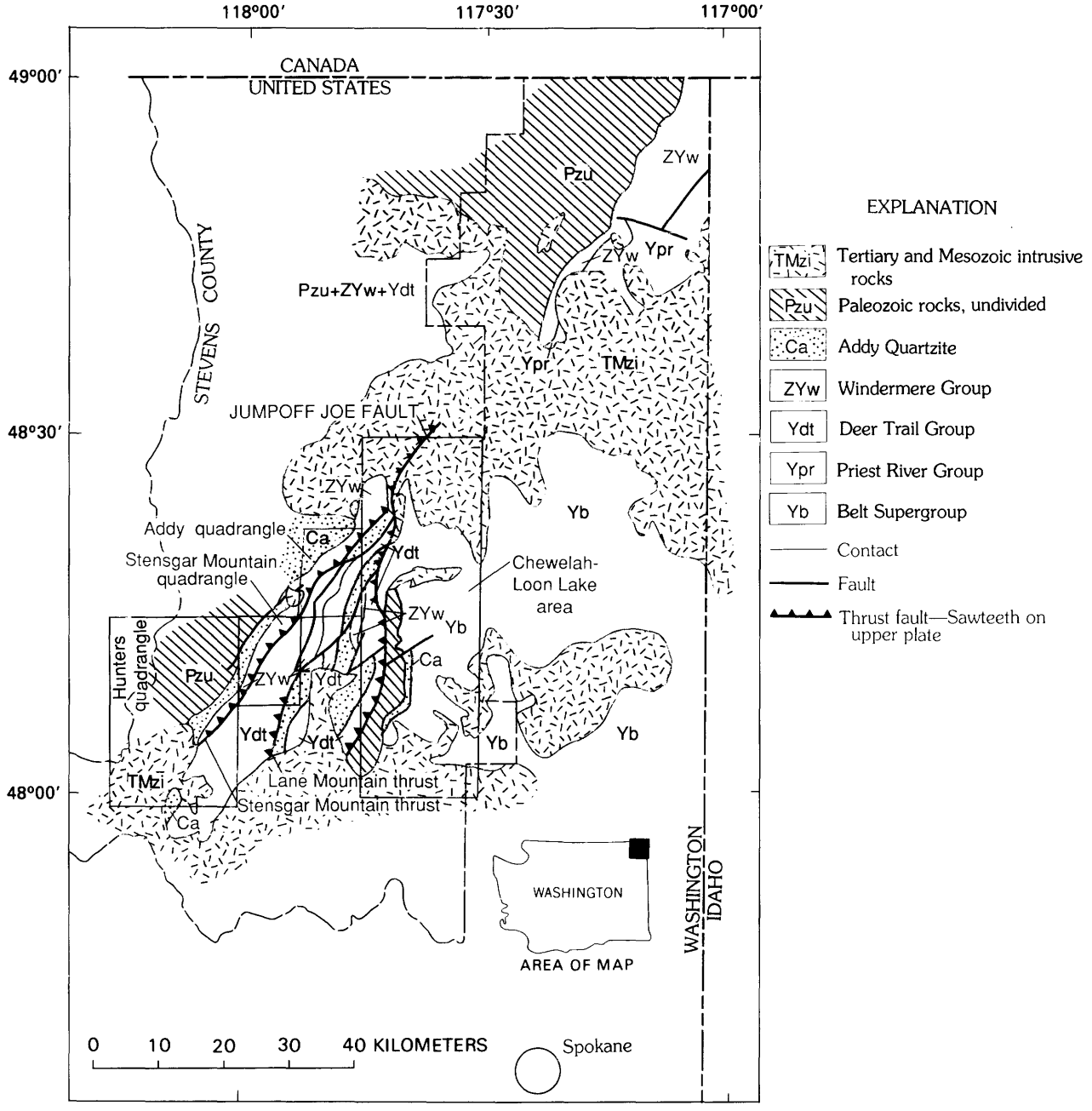

Figure 1. Index map of the study area in northern Washington, showing major geologic units and structures (modified from Miller and Clark, 1975, fig. 8).

of the major fold, however, was not located during this study, and judging from the regional geology (fig. 1), a major anticline is absent in these rocks.

Sometime after Early Cambrian time, the section composed of the Togo Formation through the Addy Quartzite underwent low-grade regional metamorphism, possibly as a result of deep burial.

The entire section of the Deer Trail Group appears to lie in a duplex fault zone (fig. 3). The Lane Mountain thrust, the floor thrust of the duplex fault zone, has the Addy Quartzite in the footwall, and so the thrusting must be post-Early Cambrian in age. The Stensgar Mountain thrust, the roof thrust of the duplex fault zone, is the contact between the Deer Trail and Windermere Groups. Low-grade dynamothermal metamorphism affected the rocks up through the Addy Quartzite and may have slightly affected the Old Dominion Limestone. During this event, the Deer Trail Group acquired slaty cleavage and was folded on macroscopic and mesoscopic scales. Minor folds and cleavage occur in the Windermere Group, and many minor folds were found in the Addy Quartzite. Cleavage generally dips steeply west, and most folds plunge at low to moderate angles north-northwest. The dynamothermal metamorphism appears to predate at least some faults in the duplex because the connecting splays between the roof and floor thrusts are undeformed. The thrusting and dynamothermal metamorphism probably occurred during the Late Triassic to Mid-Cretaceous, when rocks in northern Stevens County were similarly deformed (Mills and Nordstrom, 1979, p. 20). This timing is consistent with the Late Triassic to Cretaceous tectonism deduced for the region (Yates and others, 1966; Rinehart and Fox, 1972, p. 72; Fox and others, 1977, p. 24). The Lane Mountain pluton (161 Ma, Miller and Engels, 1975, p. 520–522; R. Fleck, unpub. data, 1987) in the adjacent Waitts Lake quadrangle (fig. 1) dates the dynamothermal metamorphism and thrusting more closely at pre-Late Jurassic (Palmer, 1983). As discussed below, the Belt Supergroup to the east probably underwent the same deformation that affected the rocks in the Stensgar Mountain quadrangle. Northeast of Chewelah, the Belt Supergroup is intruded by the posttectonic Flowery Trail Granodiorite (Miller and Yates, 1975, pl. 1), dated at 198 Ma (Miller and Engels, 1975, p. 520–522; Dalrymple, 1979) or Early Jurassic (Palmer, 1983). If at least part of the deformation in the Belt Supergroup near Chewelah correlates with deformation in the Stensgar Mountain quadrangle, the deformation in the study area occurred in Early Jurassic or Triassic.

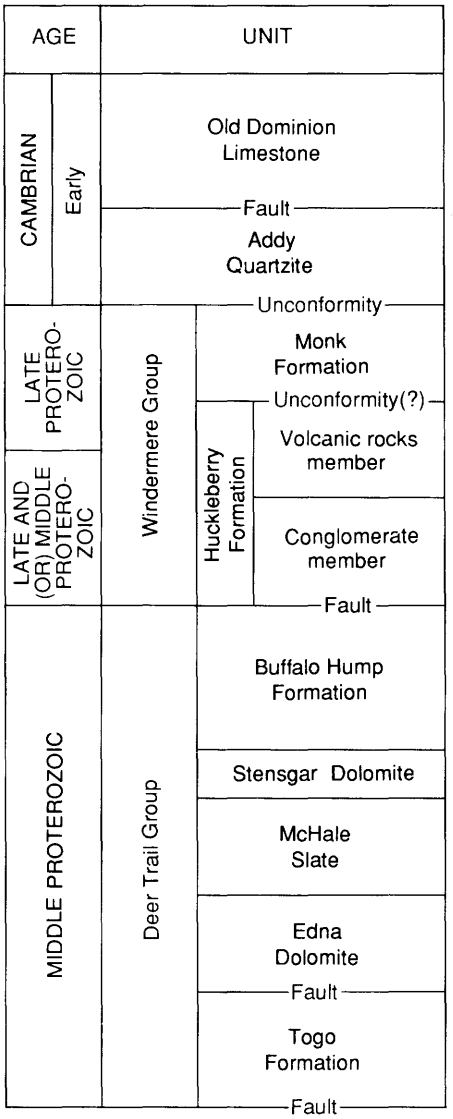

Figure 2. Stratigraphic summary of the Stensgar Mountain quadrangle (modified from Evans, 1987). Thicknesses of units are shown before Mesozoic deformation and are drawn at a scale of 1 cm = 2,000 m.

The Deer Trail Group was intruded by felsic dikes during the Mesozoic or Tertiary, and by andesite dikes possibly during the Tertiary. Glacial deposits and alluvium cover the lower elevations in the quadrangle.

DESCRIPTION OF STRUCTURES

Large Faults

Much of the structural interpretation of the Stensgar Mountain quadrangle depends on whether the contact between the Deer Trail and Windermere Groups (fig. 3) is an unconformity or a fault. Evidence bearing on these alternative interpretations is inconclusive in the study area. Fault breccia is present in poor exposures of the contact along recently constructed logging roads, but a clearly exposed fault zone could not be seen. In the Addy quadrangle (fig. 1) northeast of the Stensgar Mountain quad-

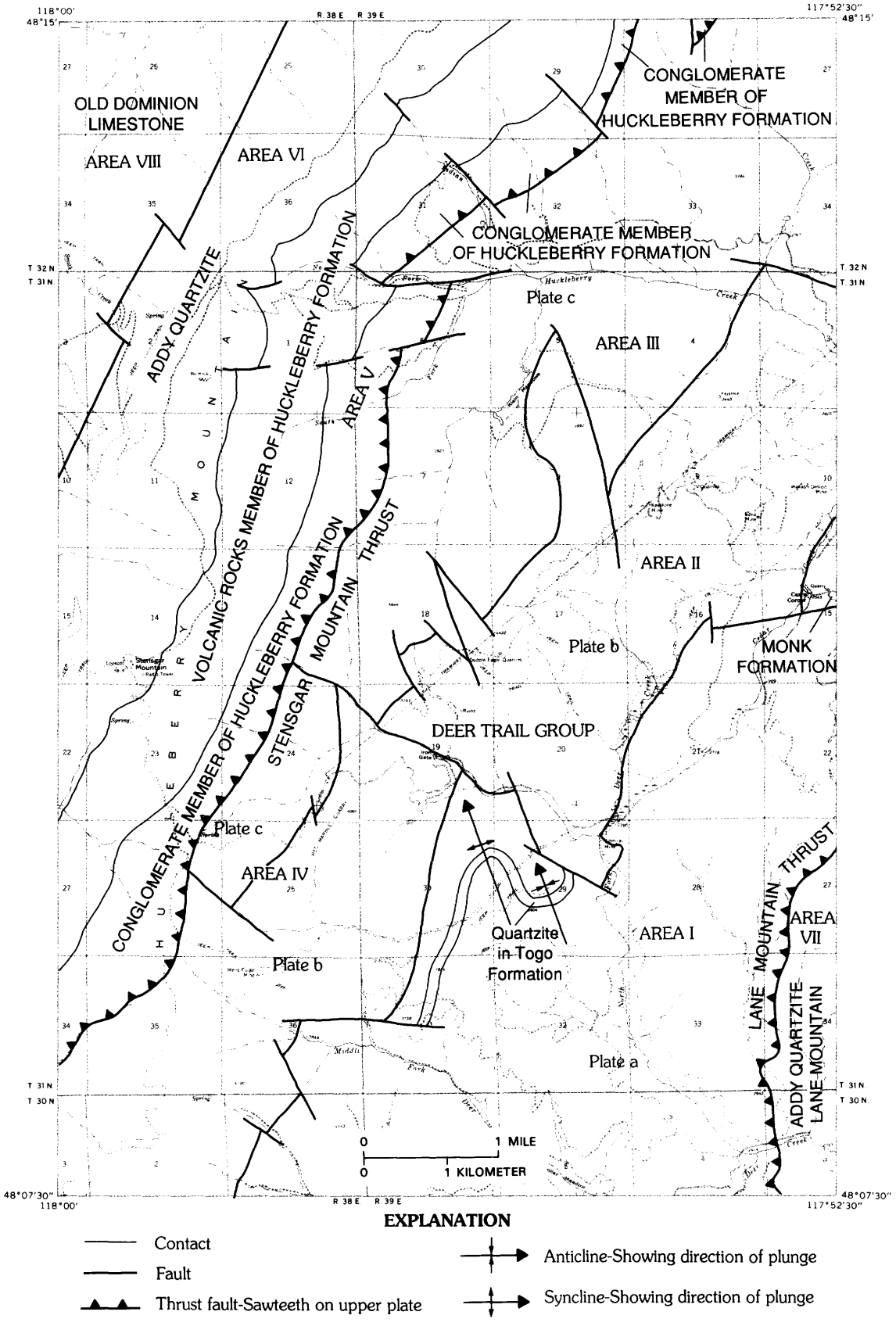

Figure 3. Geologic map of the Stensgar Mountain quadrangle. Areas I through VIII are described in text; plates a through c are structural subdivisions of the Deer Trail Group.

rangle, an extension of this contact is most likely a thrust (Miller and Yates, 1976; F.K. Miller, unpub. data, 1980). In the adjacent Hunters quadrangle (fig. 1), Campbell and Raup (1964) interpreted parts of the contact as a fault. Therefore, the contact between the Deer Trail and Windermere Groups is here interpreted as a fault in the study area and is named the "Stensgar Mountain thrust."

The Deer Trail Group appears to lie within a duplex fault zone (Boyer and Elliott, 1982, fig. 12), with the Lane Mountain thrust as the floor thrust and the Stensgar Mountain thrust as the roof thrust. Within this duplex fault zone, three thrust plates can be defined on the basis of their stratigraphy (Evans, 1987). Plate a consists of the Togo Formation. Plate b, which overlies plate a, consists of the Edna Dolomite upsection through the Buffalo Hump Formation. Plate c, which overlies plate b, consists of McHale Slate upsection through the Buffalo Hump Formation. The thrusts must have thousands of meters of stratigraphic separation. Steep northwest-striking faults cutting the thrust plates may be connecting splays between the roof and floor thrusts of the duplex fault zone (Boyer and Elliott, 1982, fig. 7).

The Lane Mountain thrust, exposed in the southeastern part of the quadrangle, underlies the entire Proterozoic and Cambrian section. The Addy Quartzite is exposed in the footwall; presumably, the Old Dominion Limestone, which should overlie the quartzite in a normal stratigraphic succession, and, possibly, even younger formations may lie beneath the thrust. The thrust is Early Cambrian or younger in age, possibly as young as Jurassic. Matrix minerals indicate greenschist-facies metamorphism of cataclasite along the margin of the hanging wall of the thrust (Evans, 1987). Thus, major movement on the thrust may have preceded or accompanied metamorphism. Cutting of the cataclasite by the thrust indicates recurrence of thrusting after the metamorphism.

Cleavage

The earliest cleavage, S_1, developed principally in argillaceous lithologies, is defined by arrays of {001} of micaceous minerals parallel to bedding (fig. 4). This cleavage probably developed during the regional metamorphism, owing to deep burial before the Proterozoic and lower Paleozoic section was tilted.

A later cleavage, S_2, also developed most conspicuously in argillaceous units, cuts across bedding at low to high angles (figs. 4, 5). This cleavage is commonly disjunctive, with smooth, sinuous traces (terminology suggested by Borradaile and others, 1982, p. 1–6). In places, the cleavage is a crenulation cleavage (fig. 4). In the argillaceous matrix of Windermere conglomerates, the cleavage commonly has rough anastomosing traces. The volume of rock occupied by the cleavage is as much as 30 percent in slate but, locally, can be much greater in rocks in which bedding

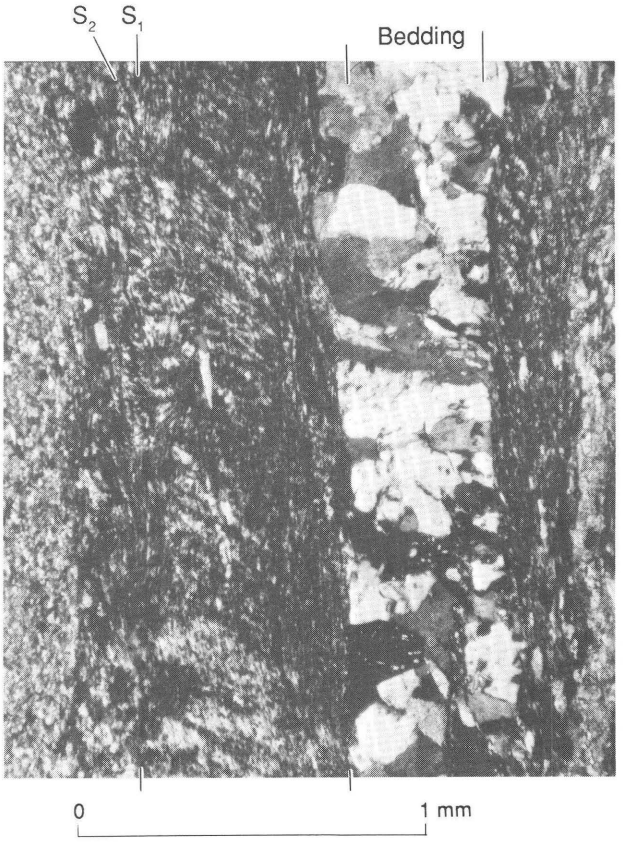

Figure 4. Early cleavage, S_1, parallel to bedding in Stensgar Dolomite. S_2, slaty cleavage.

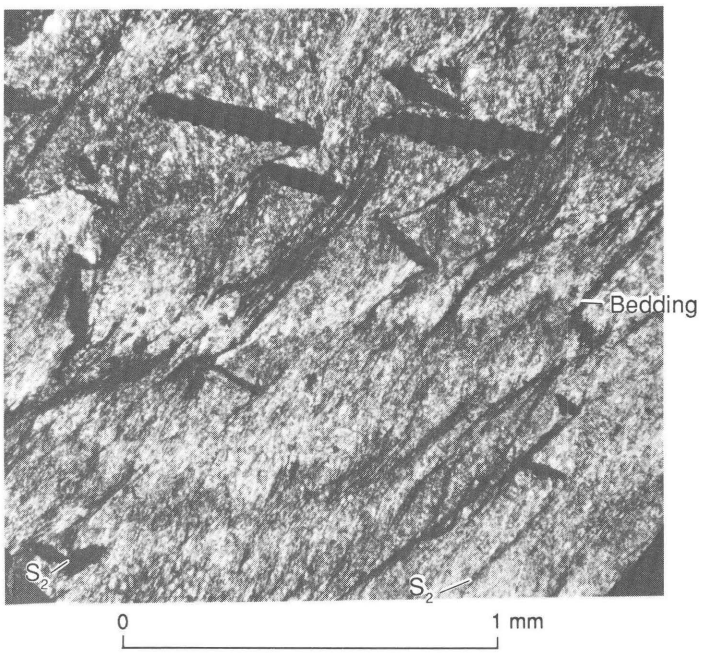

Figure 5. Slaty cleavage, S_2, cutting across bedding in slate of the Togo Formation. Opaque grains are leucoxene.

is nearly obliterated; it is much less than 30 percent in siltite, and less than 1 percent in quartzite and dolomite. Spacing of the cleavage ranges from much less than 1 mm in slate to several centimeters in siltite, quartzite, and dolomite.

Origin of the S_2 cleavage by pressure solution is indicated by truncation of quartz silt grains against the cleavage (fig. 6), by concentration of insoluble residues (opaque minerals) and mica along cleavages (fig. 7), and by stylolitic cleavage traces (fig. 8) along which insoluble residues (opaque minerals) are concentrated (see discussions of pressure solution and the origin of cleavage by Weyl, 1959; Williams, 1972, p. 35–41; Groshong, 1975, 1976, p. 1142; Rutter, 1976; Gray, 1978, p. 587–589; Kerrich, 1978; and Kerrich and Allison, 1983, p. 111).

Bedding has been deformed during formation of the S_2 cleavage in several ways. Stepped offsets of bedding along cleavage (fig. 7) are not clearly due to slip because the cleavage developed by pressure solution. Some bedding has been folded and has a closely spaced cleavage parallel to the axial planes of folds (fig. 9). In places, bedding has been nearly obliterated by a closely-spaced cleavage, leaving tightly folded remnants of beds in microlithons (fig. 10). The orientation of the folds suggests that the principal compressive stress, σ_1, was oriented at a large angle to cleavage during cleavage formation.

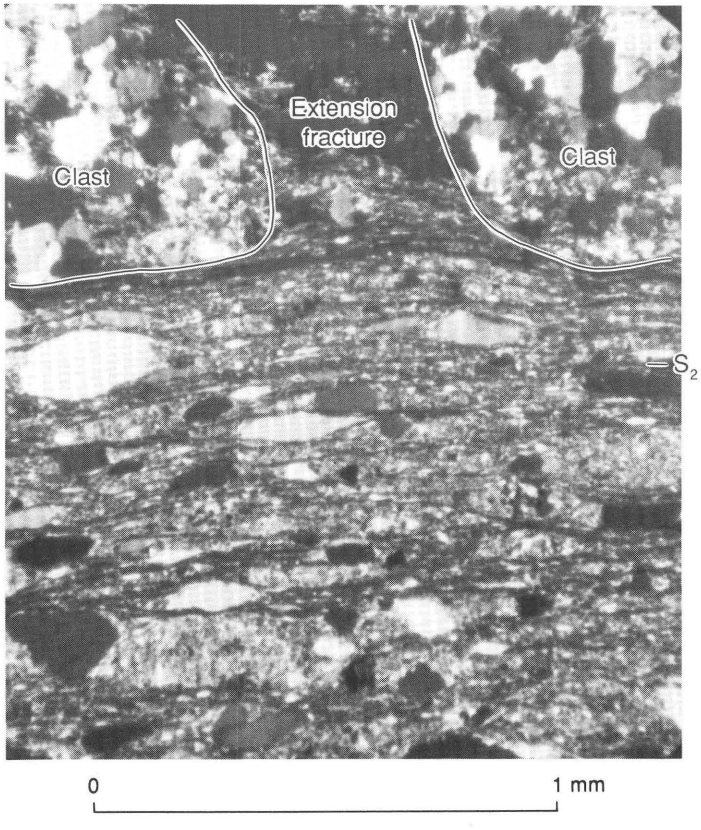

Figure 6. Slaty cleavage, S_2, in Huckleberry Formation. Truncation of quartz silt grains against cleavage suggests pressure solution. Pelitic matrix fills extension fracture in clast.

Differential movements parallel to the S_2 cleavage are suggested by clasts (fig. 11) and magnetite porphyroblasts (described below) that appear to be rotated. In figure 11, the long axis of the siltite clast is perpendicular to the cleavage, which is bent around the ends of the clast.

A late, generally steeply dipping, spaced cleavage, S_3, is present in some slates (fig. 12). These cleavages grade to discrete breccia zones, a few millimeters wide and 1 to 10 cm apart, and show apparent offsets of bedding and earlier cleavage, S_2, of as much as 5 cm. The breccia and displacements suggest shearing along S_3, although the cleavage may have originated by a nonshear process.

Slaty cleavage, S_2, suggests flattening; according to current views, cleavage forms perpendicular or approximately perpendicular to the axis of maximum finite shortening (Ramsay, 1967, p. 180; Siddans, 1972, p. 219; Wood, 1974, p. 398–399; Hobbs and others, 1976, p. 252). This interpretation is consistent with the orientations of tight folds in microlithons and of the strain indicators (clasts, ellipsoidal spots, pressure shadows, quartz-grain elongations), as described below.

Strain data from slates suggests that the minimum amount of shortening required before cleavage appears is more than 30 percent (Cloos, 1947, p. 878; Oertel, 1971, p. 536; Wood, 1974, fig. 4). Well-developed slaty cleavage, such as is generally present in the study area, reflects shortening perpendicular to cleavage by more than 50 percent (Wood, 1974. p. 399). These estimates of strain are consistent with the amount of shortening calculated from ellipsoidal spots in slate of the Buffalo Hump Formation and in slate of the Stensgar Dolomite (see below). Strain must be concentrated in the slate because of its well-developed cleavage and is much less in such rocks as Stensgar Dolomite, quartzite of the Deer Trail Group, Addy Quartzite, and the volcanic rocks member of the Huckleberry Formation, in which cleavage is poorly developed and primary textures and sedimentary structures are well preserved.

Folds

The largest clearly defined folds in the study area are an anticline and a syncline, with amplitudes of 600 m, outlined by a quartzite layer in the Togo Formation (fig. 3; Evans, 1987, pl. 1, cross sec. *C–C′*). These folds are upright and disharmonic, with slight relative thickening of quartzite in the fold hinges. The folds approximate the concentric style but have slaty cleavage in the hinge zone parallel to the axial plane of the fold and to cleavage in the slate above and below the quartzite. In parts of the hinge zone and in places on the fold limbs, bedding is transposed and paral-

lels the cleavage. The orientation of these large folds (trend, N. 20° W.; plunge, 30° NW.) is close to the attitudes of many of the mesoscopic folds associated with the slaty cleavage. Clearly, these large folds are related to the mesoscopic deformation. The faults bounding plate a (fig. 3), in which the large folds occur, appear to be unaffected by the folding. These relations suggest that the large folds and the related mesoscopic deformation of the Deer Trail Group are older than the faulting, though possibly not much older.

Large isoclinal folds may be present in parts of the Togo Formation near the Lane Mountain thrust where marker beds are absent (Evans, 1987, pl. 1, cross sec. *D–D'*). These folds are suggested by the occurrence of graded and crossbedded siltite indicating overturned bedding, near similar rocks with right-side-up bedding.

Mesoscopic bedding folds, with amplitudes ranging from 2 m (fig. 13) down to several millimeters (fig. 9), mostly in the Deer Trail Group, have disharmonic forms with relatively thickened beds in the hinge zones (figs. 14*A*, 14*B*). In figure 14*A* the folds are disharmonic, and beds apparently pinch out near one of the fold limbs; the more competent laminated zones exhibit relative thickening in the fold hinges. Most folds, whatever their size, have axial planes dipping steeply west, subparallel to slaty cleavage in the study area; and cleavage is developed in the axial zones of some of these folds (fig. 14*C*). In figure 14*C*, the concentric disharmonic folding on the west grades to a similar style on the east; beds in the anticlinal hinge are three times thicker than those in the western limb.

Axes of concentric and kink folds, with amplitudes of from 1 to 20 mm, formed in slaty cleavage parallel to bedding-cleavage intersections (fig. 7) and to cleavage-cleavage intersections (fig. 12) in argillite.

Folds in the study area are of essentially two kinds, resembling the products of the two principal fold models:

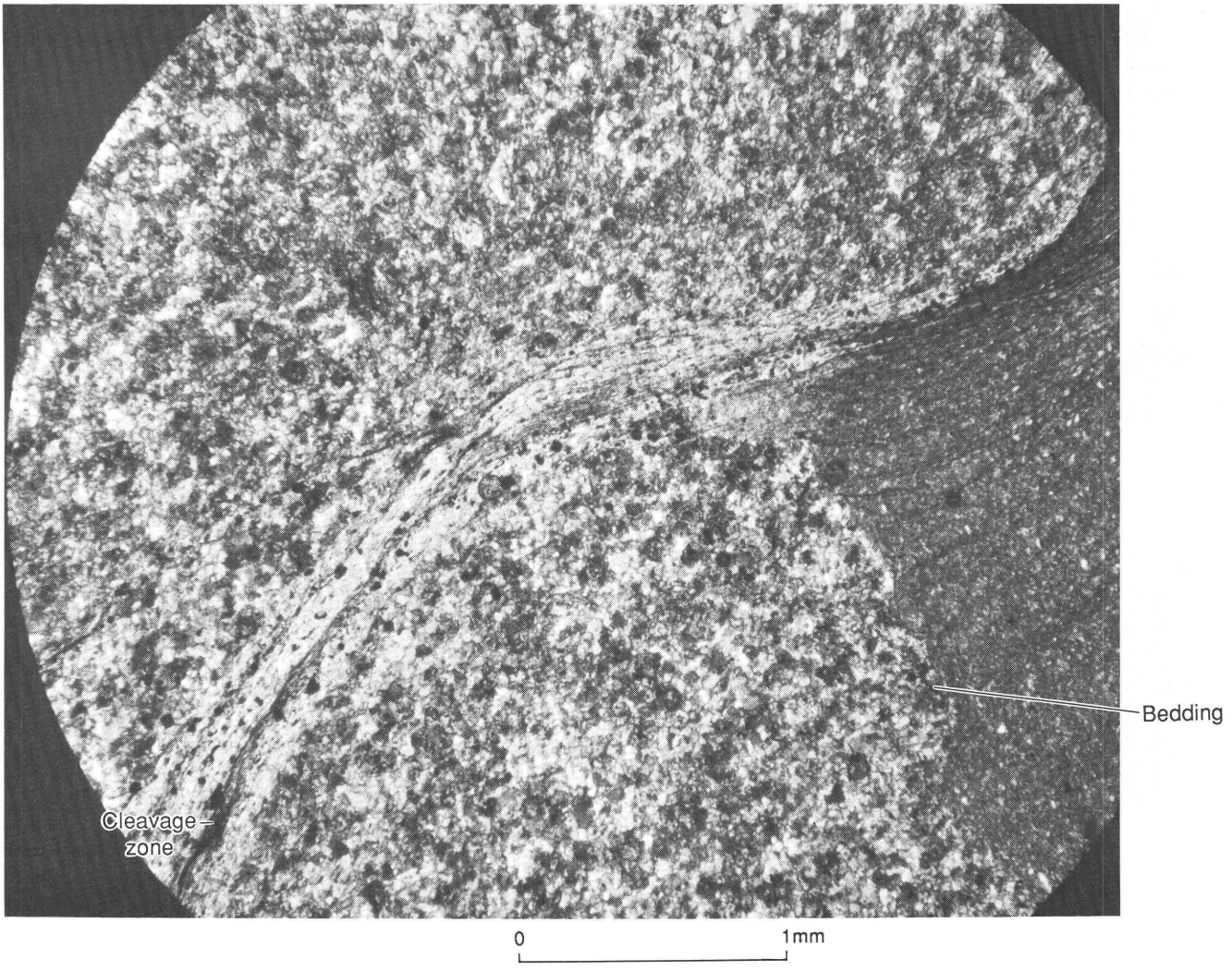

Figure 7. Concentration of mica along curved S_2 cleavage zone in Edna Dolomite. Most of the rock is silty dolomite containing abundant quartz clasts.

(1) subconcentric folds that approximate the flexural-slip folding model, and (2) similar folds that approximate the slip folding model (Turner and Weiss, 1963, p. 473–486; Whitten, 1966, p. 131–156; Ramsay, 1967, p. 392–436; Hobbs and others, 1976, p. 183–156). It is unclear, however, whether the folds in the study area formed according to these models. The actual deformational processes may have combined various mechanisms, depending on lithology or competence. For example, the subconcentric folds show evidence of slip along planes of weakness, such as bedding, at large angles to fold axes (fig. 15). In addition, the relative thickening of fold hinges suggests mass transfer either toward the fold hinges or, at least, away from the limbs, by a process not defined, or even included, in the flexural-slip model. Also, similar folds with well-developed axial-plane foliations or cleavage need not form only according to a shear model because pressure solution may also be an important process in their formation (see preceding subsection).

Figure 8. Concentration of insoluble residues (opaque minerals) along stylolitic S_2 cleavages in McHale Slate. Dolomite lens in upper right corner is truncated against cleavage.

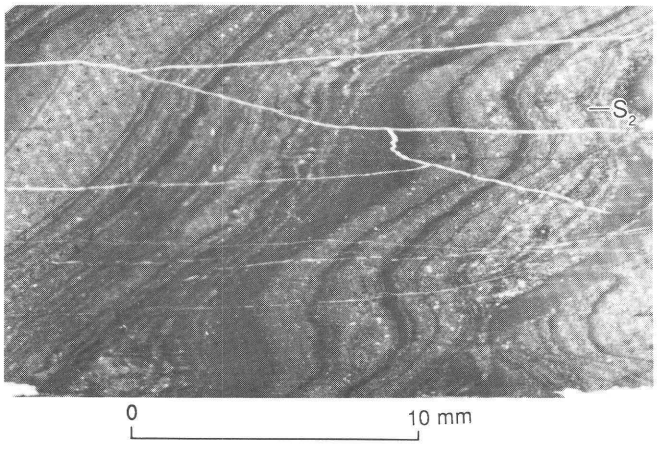

Figure 9. Slaty cleavage, S_2, parallel to axial planes of minor folds in Togo Formation. Cleavage generally is poorly developed in silty beds. Long cracks in rock parallel cleavage.

The folds shown in figure 14*C* suggest increasing intensity of strain towards the eastern part of the outcrop. The concentric fold on the west appears to grade into a similar fold on the east. Increasing strain toward the eastern part of the outcrop is also suggested by development of axial-plane cleavage, parallel to the dominant cleavage in the study area, and by relative thinning of bedding in the eastern limb (by 70 percent relative to the fold hinges and by 50 percent relative to beds to the west).

In general, style of folding is expected to vary, depending on intrinsic parameters, such as viscosity contrast and thickness of layers, and on extrinsic parameters, such as confining pressure and temperature. In figure 14*C*, pressure and temperature would probably not vary significantly across the fold. Possible chemical gradients, however, from one part of the exposure to another may affect the mineralogy and, thus, the physical properties. The dolo-

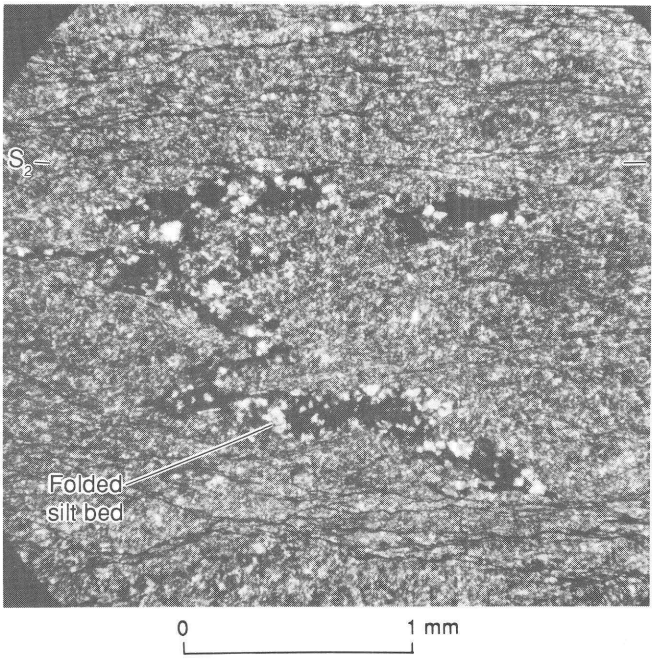

Figure 10. Tightly folded silty bed in microlithon in Togo Formation.

mite shown in figure 14*C* is locally altered to talc and serpentine. The presence of talc and serpentine could increase the rock's ductility, or the ductility could have increased during the mineralogic changes of the dolomite to calc-silicate minerals. The mineralogic changes would have been preceded or accompanied by introduction of silica into the highly magnesian dolomite. Viscosity contrast between layers could be reduced where talc and serpentine permeate the rock or are especially well developed in formerly competent layers, or it could be increased if talc and serpentine are preferentially developed in certain zones or beds. Local strains could affect the development of talc and serpentine by opening pathways for the water and silica needed for these alterations to occur in Stensgar Dolomite. The silica-bearing solutions could have formed during pressure solution in the surrounding slates.

The relation between subconcentric and similar folds illustrated in 14*C* and the parallelism of cleavage and the

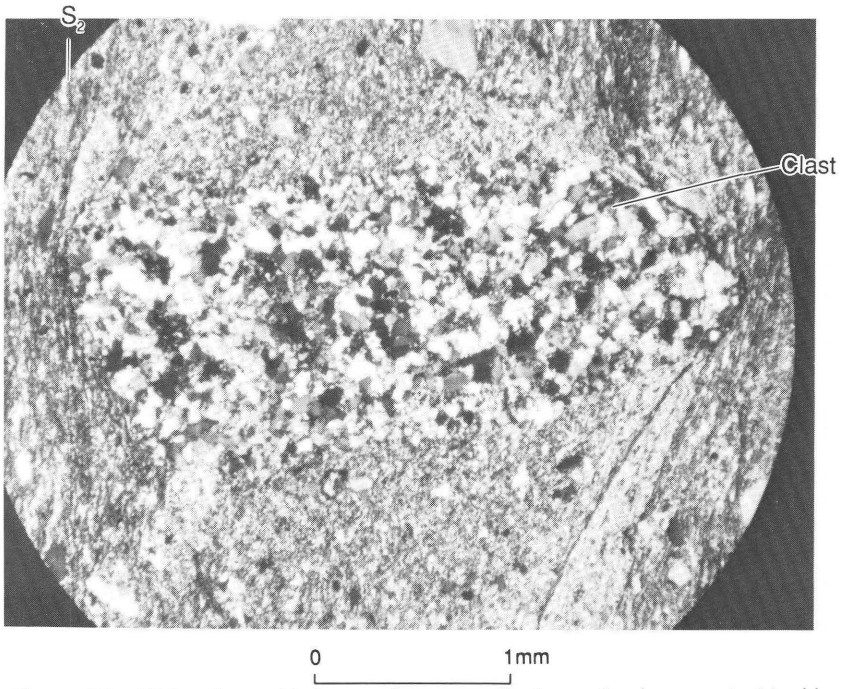

Figure 11. Siltite clast with long axis perpendicular to S_2 cleavage in Huckleberry Formation.

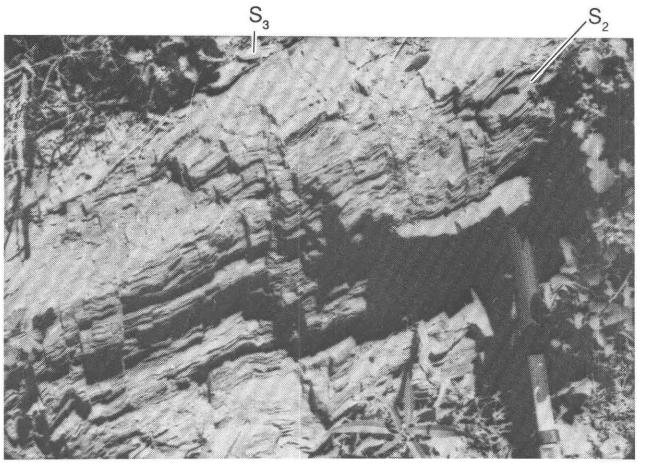

Figure 12. Fracture cleavage, S_3, cuts slaty cleavage, S_2, in Buffalo Hump Formation in SW¼ sec. 35, T. 31 N., R. 38 E. S_2 strikes northwest and dips 30° SW.; S_3 axis strikes northwest and dips nearly vertically. Hammer is 30 cm long.

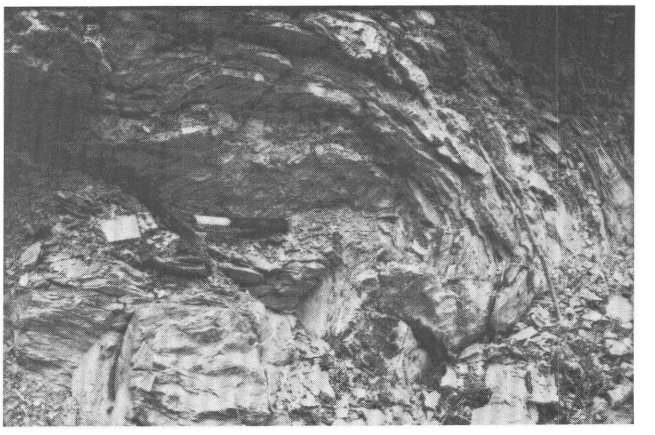

Figure 13. Fold of bedding in McHale Slate in NW¼ sec. 8, T. 31 N., R. 39 E. Handle of hammer is aligned with fold axis, which plunges 35° N. Hammer is 30 cm long.

axial planes of concentric folds, as exemplified by the large anticline in Togo quartzite suggest that the concentric and similar folds probably developed contemporaneously. In the study area, the form of a fold apparently depends on the local response to the total strain, but axial planes are at large angles to the greatest compressive strain. Theoretical justification for expecting the axial planes of concentric folds to be approximately perpendicular to the greatest total compressive strain in the rock and, therefore, approximately parallel to cleavage was suggested by Dieterich (1969, 1970) and Dieterich and Carter (1969).

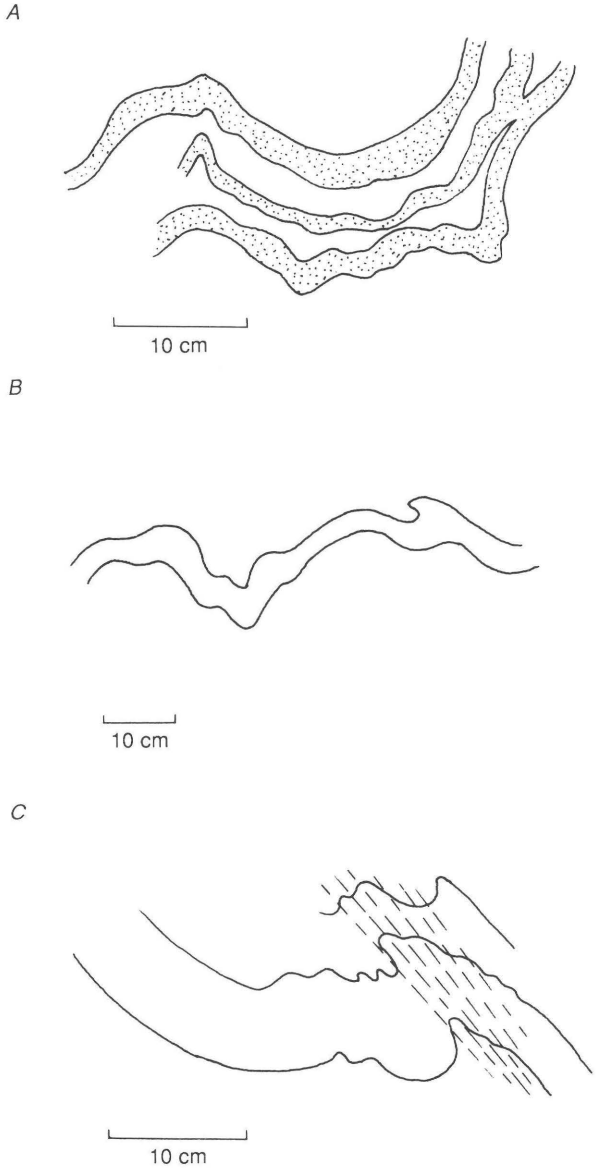

Figure 14. Folds in dolomite. *A, C,* Stensgar Dolomite in SW¼ sec. 9, T. 31 N., R. 39 E. *B,* Edna Dolomite in SW¼ sec. 30, T. 31 N., R. 39 E. Dashed lines, cleavage.

Deformed Clasts

Deformed clasts are rare in conglomerates of the Buffalo Hump and Monk Formations and the Addy Quartzite, and common in the conglomerate member of the Huckleberry Formation. In the Buffalo Hump Formation, a conglomerate in the NE¼ sec. 3, T. 30 N., R. 38 E., in the southwest corner of the quadrangle contains quartz, quartzite, and quartz siltite clasts, the long axes of which lie in the plane of a pervasive cleavage in the matrix. These clasts are elongate as much as 4:1 (fig. 16) at a small angle to north-northwest-trending fold axes in the study area. In thin section, some of the quartzite and quartz siltite clasts have sedimentary textures internally, and so they must have undergone little or no internal deformation. Although the elongate shapes of these clasts could be primary, their parallelism with cleavage and near-parallelism with fold axes suggests that the elongation is largely tectonic, possibly due to tectonic enhancement of a weak sedimentary fabric. Clasts may have attained their present shapes and orientations by rotation, pressure solution, and (or) tectonic abrasion. Evidence for pressure solution is the truncation of clasts along cleavages, which are marked by concentrations of iron oxide (insoluble residues) and interpenetration of clasts (fig. 17).

The conglomerate member of the Huckleberry Formation contains quartz, siltite, argillite, and dolomite clasts that are flattened in a plane parallel to slaty cleavage of the argillaceous matrix. Some clasts are elongate as much as

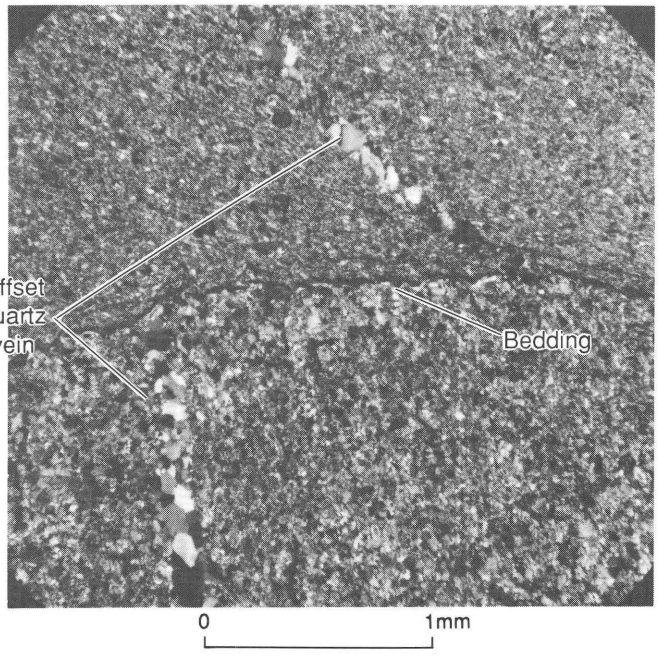

Figure 15. Quartz vein offset along bedding in Edna Dolomite; offset vein generally parallels S_2 cleavage in the rock.

5:1 (fig. 18) at a small angle to fold axes in the study area. Slate clasts, the most abundant kind, are commonly less than 1 mm thick. Aalto (1971, p. 760) observed that the clasts in undeformed (uncleaved) conglomerate stratigraphically equivalent to the conglomerate member of the Huckleberry Formation show no preferred orientation. Ross and Barnes (1975, p. 194), however, found that the clast orientations in some undeformed conglomerate from this same unit in southeastern British Columbia define a weak planar fabric. The longest axes of these quartzite clasts form a diffuse concentration plunging at low to moderate angles generally northeast, with a mean plunge of north-northeastward. This primary fabric suggests that the strong dimensional fabric of clasts in the Stensgar Mountain quadrangle is largely of tectonic origin, but strongly influenced by primary clast shape and orientation. Some clasts may have attained their present dimensions and orientations by the processes suggested above for conglomerate of the Buffalo Hump Formation (rotation, fig. 11; pressure solution, fig. 6; tectonic abrasion). The flattened siltite clasts shown in figure 18 appear to have sedimentary textures internally and thus may have been little affected by plastic deformation; however, plastic deformation of some slate clasts cannot be ruled out. Some slate clasts have a composition approximately like that of the matrix and would be expected to behave like the matrix during deformation, given similar lithification of both matrix and clasts. Some slate clasts, possibly differing from the matrix in degree of lithification, underwent late brittle extension (fig. 19). Presuming that the flattening occurred several hundred million years after deposition, the ductility contrast between the matrix and most slate clasts quite probably was small before deformation. The slate clasts, therefore, could serve as qualitative strain markers in the rock, keeping in mind that their original sedimentary shapes may have been discoid. The extreme thinness of many slate pebbles strongly suggests that the unit as a whole underwent a predominantly flattening deformation, with the maximum principal compressive-strain axis oriented perpendicular to cleavage. Some strain could have occurred during deep burial of the conglomerate under at least 5.5 km of overlying Proterozoic and Lower Cambrian deposits (see formation thicknesses in table 1 of Evans, 1987). This portion of the total strain is not easily separated from the later strain that dominates the fabric in the lower part of the Huckleberry Formation.

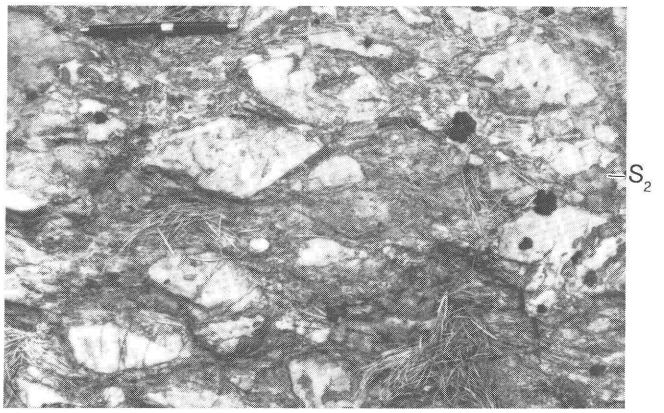

Figure 16. Deformed clasts in Buffalo Hump Formation in NE¼ sec. 3, T. 30 N., R. 38 E. View is perpendicular to clast elongation. Pen is 13 cm long.

Some clast elongation in the Huckleberry Formation is due to pulling apart (figs. 18–20). Tension fractures within clasts are oriented at large angles to matrix cleavage, and the extension direction (pole to tension fractures) is in or close to the plane of cleavage and subparallel to the long dimensions of the clasts. The clasts have evidently deformed in a brittle mode, whereas the matrix deformed in a ductile mode—a difference implying a significant ductility contrast between pebbles and matrix, even for some slate pebbles, during this part of the deformation (fig. 19). Ross and Barnes (1975) reported clasts with tension fractures at large angles to slaty cleavage and perpendicular to later fracture cleavage in a British Columbian conglomerate correlative with the Huckleberry Formation. However, a late fracture cleavage normal to tension fractures is absent in the Huckleberry Formation. In most pebbles in the study area, the tension fractures in clasts are conspicuous because the material that occupied the fractures was removed during weathering. In figure 20, parts of the fractures are still filled with quartz. In figure 6, remnants of the filling suggest that the fractures were filled with the rock's matrix, forming boudinage. Basal cleavages of micaceous minerals in these fractures are perpendicular to the fracture walls. The cumulative widths of tension fractures in the clasts provide a minimum estimate for the amount of elongation of the rock as a whole associated with this semibrittle component of the deformation. The slate and siltite clasts shown in figures 18 and 19 are pulled apart 14 and 19 percent, respectively; the quartz pebble in figure 20 is pulled apart 8 percent. Tension fractures are not present in all clasts. Insufficient information is available to determine whether clast tension fractures occur preferentially in certain parts of the study area.

Conglomerate in the Monk Formation in the NE¼ sec. 15, T. 31 N., R. 39 E., contains clasts, chiefly of slate, and subordinate amounts of pebbles of siltite, dolomite, and quartzite. Some well-rounded quartzite cobbles in the formation appear to be undeformed (Evans, 1987, fig. 10). Clasts of argillite and, to a lesser extent, siltite and dolomite are flat parallel to slaty cleavage. Here, bedding and slaty cleavage are about parallel. The slate clasts are less than 1 mm thick and are elongate as much as 4:1 in a consistent direction, parallel to local minor crenulations (fig. 21)—

features suggesting that this well-developed dimensional fabric probably has a large tectonic component.

Quartzite and quartz siltite clasts in a conglomerate lens in the Addy Quartzite in the SE¼ sec. 22, T. 31 N., R. 38 E., are flat parallel to a locally developed cleavage and elongate as much as 2:1 subparallel to minor fold axes in nearby quartzite.

Sand-size quartz clasts in quartzite beds in the Togo and Buffalo Hump Formations and in the Addy Quartzite show varying amounts of strain, including flattening of grains parallel to a local slaty cleavage (Togo and Buffalo Hump Formations), or in zones oriented at an angle to bedding (Addy Quartzite, fig. 22). Many of these grains also exhibit undulatory extinction, polygonization, deformation lamellae, and recrystallization. Some strain features, excluding dimensional flattening, may be inherited from the source terrane of the clasts, but part of the internal strain is probably related to inplace flattening of the grains.

Deformed clasts in conglomerates of the study area are flattened parallel to slaty cleavage. The longest dimensions of these clasts are generally at a small angle to fold axes and crenulations in nearby rocks. If the clasts are qualitative strain indicators, their shapes imply a geometry of maximum elongation that does not correspond to what has

Figure 17. Pressure solution indicated by interpenetration and truncation of clasts and concentration of insoluble residues (iron oxides) along S_2 cleavage in Buffalo Hump Formation.

been found in some other studies. Strain analyses of ooids by Cloos (1947, 1971) and of ellipsoidal strain indicators by Wood (1973) lead to conclusions that minimum extension occurs parallel to fold axes and that maximum extension occurs perpendicular to fold axes. Although similar conclusions were drawn from experiments in rock deformation (Patterson and Weiss, 1966; Hobbs and others, 1976, p. 285), Ramsay (1981) described maximum extension at a large angle to fold axes low in the pile of Helvetic nappes, and parallel to fold axes in structurally high nappes. Avé Lallemant (1979) noted principal extension in the northern Sierra Nevada parallel to steeply plunging lineations and fold axes during the Triassic and Early Jurassic, and at high to moderate angles to fold axes during the Late Jurassic. Byrne (1984) described extension parallel to folds in a tectonic belt in the Kodiak Islands. Snook and others (1982), Ellis and Watkinson (1987), and Watkinson and Ellis (1987) mentioned maximum extension parallel to fold axes in northeastern Washington. Ross and Barnes (1975, p. 1293) found long axes of deformed clasts parallel to fold axes in diamictites of southeastern British Columbia.

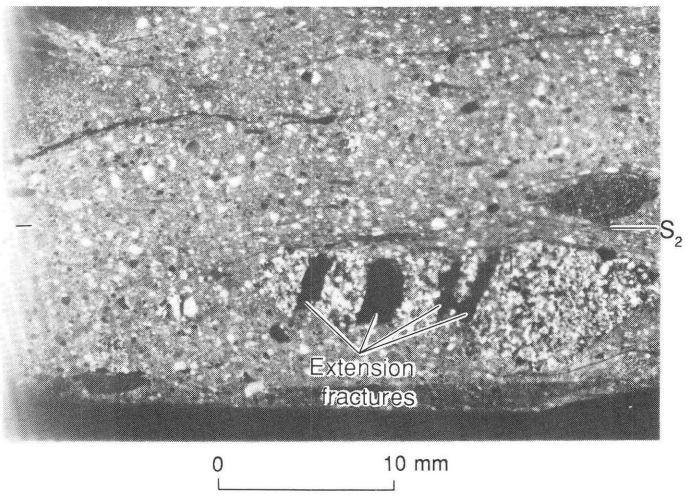

Figure 18. Flattened and pulled-apart pebble in Huckleberry Formation. Remnant material in crossfractures (black bars across pebble; fracture fillings mostly plucked during grinding) resembles micaceous matrix of the rock.

Several hypotheses may explain the angular relations of clast elongations and fold axes in the Stensgar Mountain quadrangle. (1) Clast shape was influenced by a primary sedimentary fabric that was more strongly developed in the study area than elsewhere. (2) Clasts were stretched parallel to a local direction of maximum elongation that does not parallel the maximum elongation of the mean strain ellipsoid. (3) Fold axes formed at large angles to the direction of maximum elongation marked by clast elongation, and were rotated toward the direction of clast elongation. (4) Clasts were rotated toward alignment with fold axes.

Figure 19. Elongate clasts in Huckleberry Formation near ctr. sec. 31, T. 32 N., R. 39 E. Veins crossing pebble axis (dark lines) are weathered out. Pen is 13 cm long.

Although mean strain for the study area does not require that fold axes be oriented in any particular direction to maximum elongation of the mean strain ellipsoid, the axes and long dimensions of clasts generally lie in the mean plane of flattening. The field and laboratory studies cited above, however, suggest that fold axes and clast elongations can be expected to have specific angular and kinematic relations. Inasmuch as so many factors affect the orientations of folds and the long dimensions of clasts, an explanation for the angle between fold axes and clast elongations probably cannot be easily inferred from the clast fabric in the Stensgar Mountain quadrangle.

Similarity in orientation of the long axes of clasts and other indicators of extension described here and below (necking in dolomite, elongation of pressure shadows, and pulled-apart clasts) suggests that clast elongations in the Addy Quartzite, Buffalo Hump Formation, and Windermere Group record a large component of principal elongation in the rock. Hypothesis 3 of the preceding paragraph may be the best explanation for the angular relations of some fold axes and elongated clasts, as suggested by the rectangular relation of crenulations and extension direction in the dolomite lens described below. For other clasts, possibly with a primary sedimentary fabric, a linear dimensional fabric subparallel to fold axes may have developed, and both fold and clast axes were subsequently rotated toward the direction of maximum elongation in the rocks. This hypothesis seems consistent with crenulations parallel to clast elongations in the Monk Formation. The mechanisms controlling the angular relations of fold axes and clast elongations may vary in the study area, but the controlling factors are not clear.

Pressure Shadows

Euhedral and subhedral porphyroblasts of magnetite and pyrite, with pressure shadows of quartz, biotite, and carbonate, are present in some metabasalt dikes and in some slate of the Deer Trail Group. Locally, as illustrated

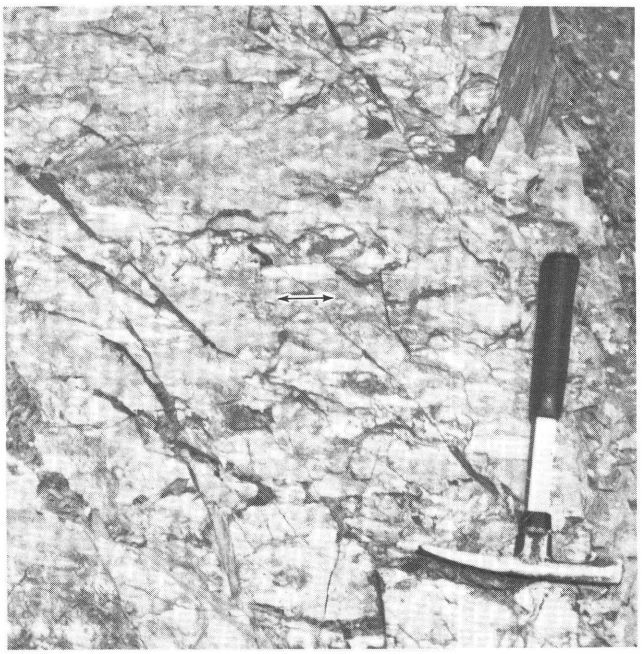

Figure 21. Elongate annd flattened pebbles in Monk Formation in NW¼ sec. 5, T. 31 N., R. 39 E. Arrow denotes trend of crenulations on cleavage surface. Hammer is 30 cm long.

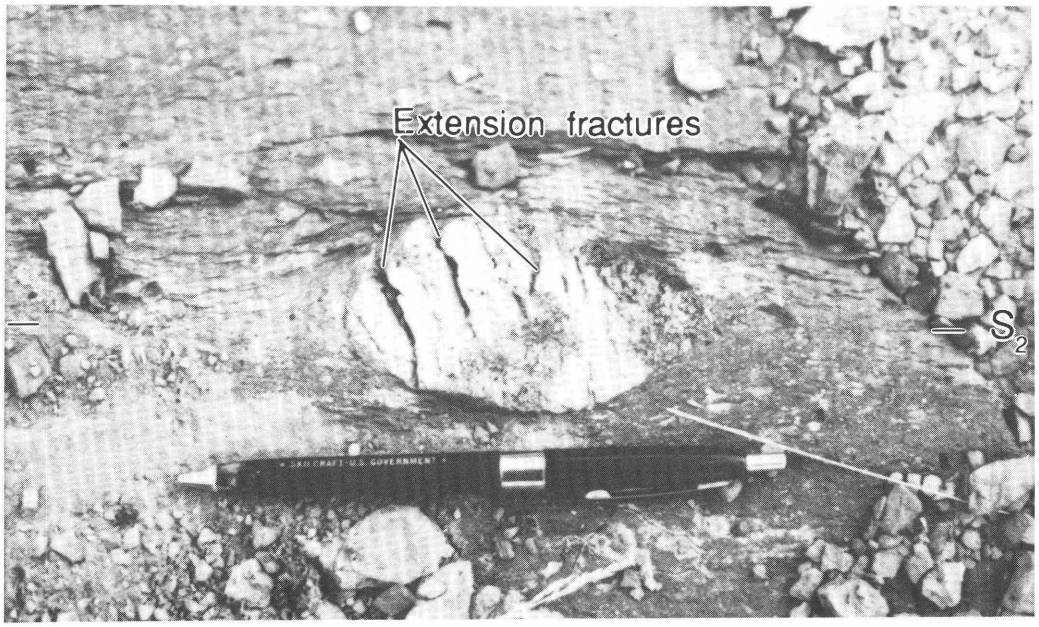

Figure 20. Pulled-apart quartz clast in Huckleberry Formation in SE¼ sec. 34, T. 31 N., R. 38 E. Pen is 13 cm long.

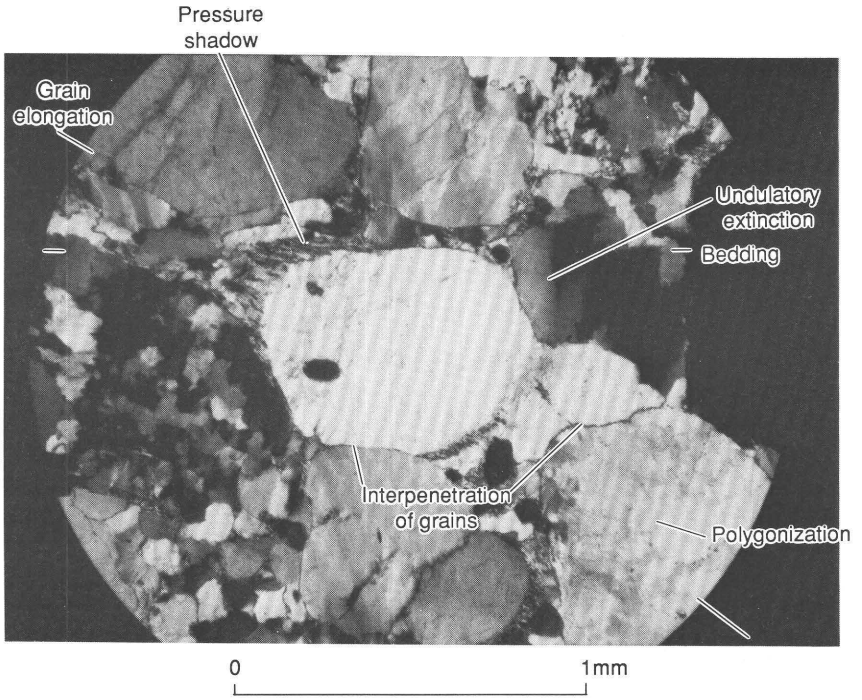

Figure 22. Deformed quartz grains in Addy Quartzite. Larger grains are elongated at 25° angle to bedding. Slight interpenetration of grains indicates pressure solution. Thin pressure shadows (quartz beards) are developed along edges of some grains.

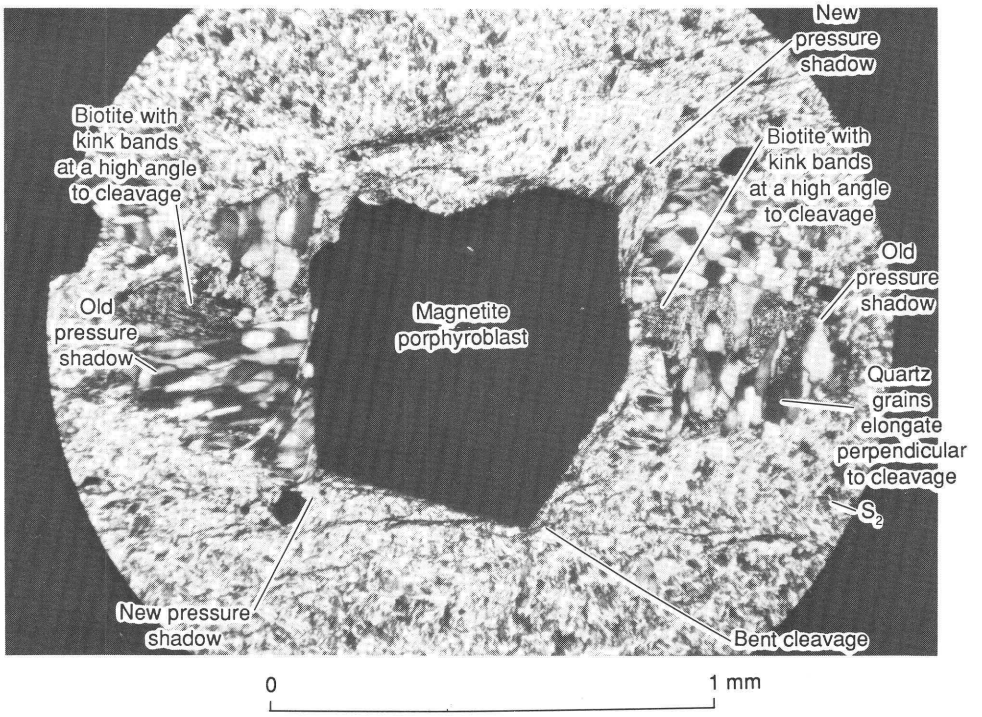

Figure 23. Magnetite porphyroblast in Togo Formation, with pressure shadows of quartz and biotite. S_2, slaty cleavage.

in figure 23, apparent bending of cleavage around some porphyroblasts suggests that the porphyroblasts continued growing after cleavage was formed. Elongation of the pressure shadows parallel to the cleavage suggests that the pressure shadows formed during cleavage development (fig. 23). The pressure shadows in sections perpendicular to the local crenulations, in the S_2 cleavage are longer than in sections parallel to the crenulations, a relation suggesting that the principal elongation in the rock is perpendicular to the crenulations (fig. 24) and that the deformation is characterized by flattening in the plane of cleavage.

Within the pressure shadows shown in figure 23, some quartz grains are elongate parallel to slaty cleavage, whereas others are elongate perpendicular to cleavage. Biotite grains in the central parts of the pressure shadows have {001} parallel to cleavage and have kink bands. Wedges of the micaceous matrix of the argillite intrude between the pressure shadows and the porphyroblasts, partly separating the porphyroblasts from their pressure shadows.

Elongate quartz grains in pressure shadows (fig. 22) can be viewed as a result of preferential grain growth in a direction parallel to the least principal stress at the growth surface (Durney and Ramsay, 1973, p. 83), with the constituents of the growing grains derived from pressure solution of minerals in the surrounding rock. These processes would be consistent with the development of pressure shadows parallel to slaty cleavage in the study area and the elongation of quartz grains in the pressure shadows parallel to cleavage shown in figure 23.

The quartz grains elongate perpendicular to the pressure shadows shown in figure 23 appear to contradict this model. One explanation of this apparent inconsistency is suggested by biotite kink bands in the pressure shadows: These bands are oriented at large angles to cleavage and to the long dimensions of the shadows. Experimentally produced kink bands in biotite have been found only in grains with {001} inclined at low angles to the maximum-principal-compressive-stress axis, σ_1 (Turner and Weiss, 1963, p. 358); the poles of these kink bands are close to σ_1. According to this criterion, the kink bands shown in figure 23 must

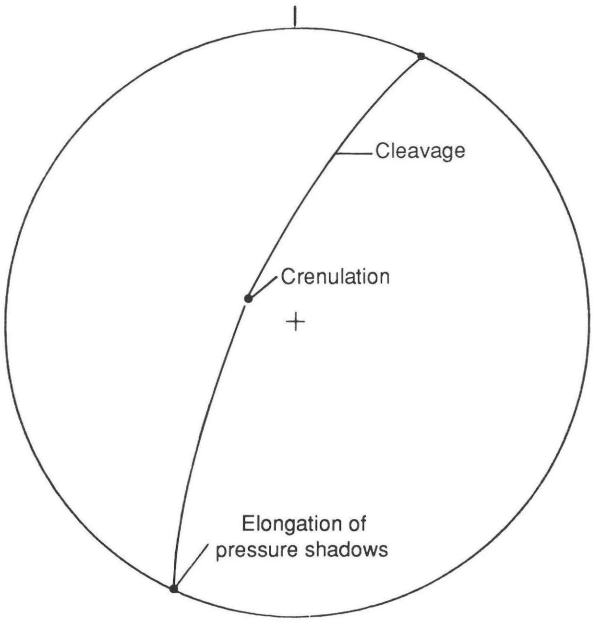

Figure 24. Orientation diagram of structural elements in sample shown in figure 23.

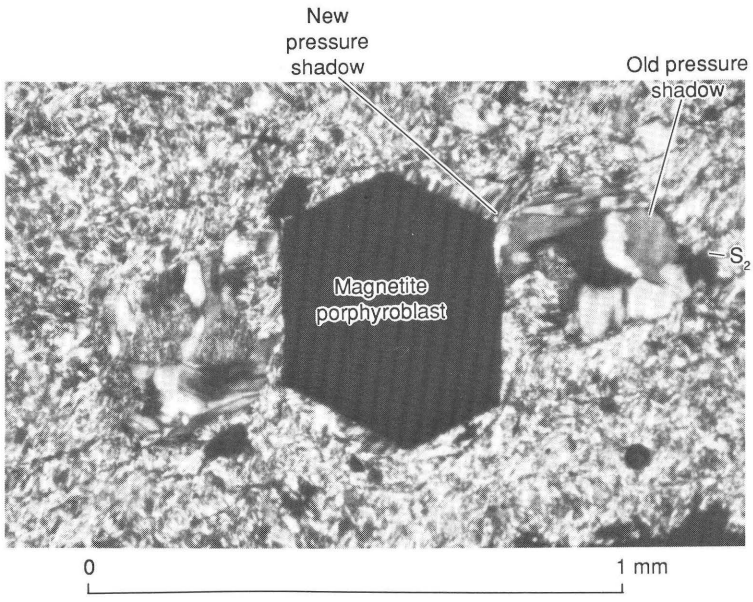

Figure 25. Magnetite porphyroblast in Togo Formation separated from its old pressure shadow. S_2, slaty cleavage.

record the effect of a later stress oriented at nearly right angles to the stress that dominated during formation of the slaty cleavage. Such a stress, which may have existed long enough to influence the growth of quartz grains at right angles to cleavage, could have arisen owing to elastic recovery after the main phase of deformation (Tobisch and Fiske, 1976, p. 1419).

The magnetite porphyroblast in figure 25 is almost completely separated from its old pressure shadow by pelitic matrix. The porphyroblasts shown in figures 23 and 25 have small new quartz pressure shadows at acute angles to cleavage. These new pressure shadows probably reflect a later, weaker strain after the principal stage of deformation during which the S_2 cleavage formed. No cleavage younger than S_2, however, was found in this rock.

Quartz Veins

Quartz veins, as much as several centimeters wide, are locally abundant in the Deer Trail Group, especially in the Edna Dolomite, and are locally abundant in the Addy Quartzite. Many of these veins are oriented at large angles to slaty cleavage and may be tension fractures formed during a late brittle stage of deformation. Other veins may occupy shear fractures; some veins parallel cleavage. Veins parallel to cleavage are commonly nodular, with locally well developed crenulations along the margins and local buckling (fig. 26). Their occurrence implies rotation of early-formed quartz veins into parallelism with cleavage, or late extension perpendicular to cleavage, inasmuch as quartz veins would probably not form parallel to cleavage while maximum compression was oriented perpendicular to cleavage. These veins, like the complex pressure shadows shown in figure 23, could be recording one or more episodes of elastic recovery (Tobisch and Fiske, 1976, p. 1419).

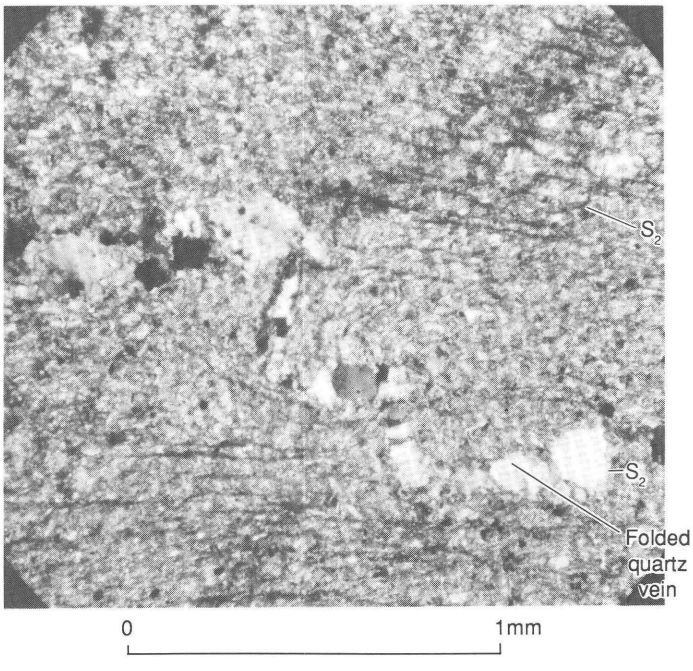

Figure 26. Folded quartz vein in Edna Dolomite. Vein parallels S_2 cleavage in most of sample.

Ellipsoidal Spots

Pale-brown and pale-green ellipsoidal spots, as much as 5 cm long, occur in gray argillite of the Buffalo Hump Formation in the NW¼ SW¼ sec. 9, T. 31 N., R. 39 E. Most of these spots have brown cores, as much as 1 cm across. Some ellipsoids have major and intermediate axes along planes oriented at 0° to 4° to slaty cleavage and are elongate parallel to microcrenulations of the cleavage, whereas others are elongate at other angles (15°–80°) to the microcrenulations. Similar ellipsoids in Wales were studied by Wood and Oertel (1980, p. 313), who found that the ellipsoids contain less iron (oxidation state unchanged) and manganese and more calcium and boron than the surrounding rock, owing to diagenetic diffusion. These ellipsoids can be used as strain markers if the ellipsoids were spherical before deformation or if stages in their strain history can be identified. The ellipsoids in the Stensgar Mountain quadrangle may not have been spherical before the Mesozoic deformation because this event was preceded by deep burial of the Buffalo Hump Formation, when the spots may have been initially deformed. Departure from initial sphericity before development of the slaty cleavage, or a complex deformation path, may be reflected in the small angle between cleavage and the plane of apparent flattening of some ellipsoids, the shortest axes of a few ellipsoids in the plane of cleavage, and the varying angle between microcrenulations and long axes.

The ellipsoids may also have undergone a volume reduction by loss of water and soluble constituents. Initial volume loss occurred during sedimentary compaction and could have been as high as 50 percent (Beutner, 1978, p. 18–19; Wright and Platt, 1982, p. 129). Initially spherical reduction spots would have assumed the shape of oblate spheroids, with short axes perpendicular to bedding. Ramsay and Wood (1973, p. 267) estimated a possible volume loss of 10 to 20 percent in the conversion from lithified mudstone to slate, and a volume loss of more than 20 percent if the initial material was incompletely consolidated sediment. Deep burial of the rocks by Early Cambrian time and their possible subjection to low-grade metamorphism owing to deep burial during the early Paleozoic indicate that the Buffalo Hump Formation was well lithified by the Mesozoic. These relations suggest an upper limit of 20-percent volume reduction during the Mesozoic deformation.

If the highly cleaved rocks lost as much as 70 percent (compaction plus deformation) in volume, evidence for the transport and deposition of such a large volume of material is absent. Much of the volume change (50-percent compaction) probably occurred while the units were part of an open system. Much of the silica lost from the Deer Trail Group at that time may have been deposited as quartz cement in the Addy Quartzite. The present occurrences of quartz veins and quartz pressure shadows in the Deer Trail Group, and silicic phyllite zones in the volcanic rocks member of the Huckleberry Formation are more consistent with a volume loss of less than 20 percent associated with the Mesozoic dynamothermal metamorphism.

Despite the uncertainties of strain history noted above, calculations of shortening and elongation of several ellipsoids were made, assuming initial sphericity and a total of 20 percent volume loss, to estimate the total strain in the rock, regardless of when each strain increment occurred (table 1). Knowledge of the intermediate shapes and orientations of the ellipsoids is important because superposed strains can give the final ellipsoid a shape that may not closely match the total mean strain ellipsoid of the Mesozoic deformation. Here, because compaction and shortening perpendicular to cleavage are both at large angles to bedding, both of these major strain events may have been nearly coaxial with respect to the axis of principal shortening, and so their additive strains may be much greater than other, smaller magnitude noncoaxial strains that the rocks may have undergone. The effect of compaction and tilting of the rocks before dynamothermal metamorphism, however, would cause the final ellipsoidal spots to have axes that do not accurately reflect the final strain event (dynamothermal metamorphism). This mismatch of axes may be reflected in the small (0°–4°) angle between elongate axes of ellipsoids and cleavage, the wide variation in the shapes of ellipsoidal spots, and, possibly, also the 0°–80° range in the angle between long axes of spots and microcrenulations on the S_2 cleavage. At the large strains involved, the mismatch of axes is not large, but the magnitude of the maximum extension may be less than the amount suggested by the ellipsoids. If intermediate strains included layer-parallel shortening before dynamothermal metamorphism, elongation could have been greater than suggested by the ellipsoids. The amount of shortening suggested by the ellipsoids is 40 to 78 percent (avg 67 percent); maximum elongation in the cleavage would be 152 to 252 percent (avg 200 percent). The intermediate axes appear to be relatively shortened (max 36 percent) or relatively elongated (max 163 percent), with an average length change of 124 percent.

The ellipsoids were not found in place, and so the orientations of elongations of ellipsoids cannot be compared directly with those of other linear structural elements. However, if the crenulations on the cleavage of the rocks containing the ellipsoids are parallel, the ellipsoids consist of at least two populations: (1) ellipsoids with long axes parallel to microcrenulations and to each other, and (2) ellipsoids that appear to have a random orientation of long axes in the plane of cleavage. If the microcrenulations are subparallel to most linear elements in the quadrangle, they and the long axes of the first group of ellipsoids plunge at low to moderate angles north-northwest. The randomly oriented ellipsoids probably reflect complex deformation paths that cannot be sorted out with the information available.

Table 1. Percent strain calculated from ellipsoidal spots
[n.m., not measurable]

Spot	Angle between X and crenulations	X	Y	Z
	Buffalo Hump Formation			
A	0	1.95	1.25	0.23
B	0	1.73	1.18	.25
C	0	1.88	.86	.50
D	0	2.36	.75	.47
E	0	2.11	.64	.60
F	80	2.42	1.49	.22
G	40	2.52	1.33	.24
H	40	1.92	1.25	.34
I	55	1.90	1.43	.30
J	30	1.76	1.37	.33
K	15	1.86	1.40	.31
L	25	1.63	1.63	.30
M	45	1.52	1.52	.35
N	55	2.44	1.25	.26
O	65	n.m.	n.m.	n.m.
P	50	n.m.	n.m.	n.m.
	Stensgar Dolomite			
Q	0	1.41	0.81	0.50
R	0	2.41	.78	.30
S	0	1.69	.87	.39
T	0	2.05	1.02	.27

Ellipsoids in slate of the Stensgar Dolomite were found in place outside the study area in a roadcut about 2 km southwest of Chewelah (see Miller and Clark, 1975, pl. 1). The long axes of these ellipsoids parallel microcrenulations and plunge at low angles north.

The axes of four ellipsoidal spots in a hand specimen of slate from the Stensgar Dolomite were measured, and the strains calculated from these measurements (table 1). Average shortening is about the same (63 percent) as for spots in the Buffalo Hump Formation. Maximum elongation averages a little less (189 percent) than for the Buffalo Hump of the study area. The intermediate strain axes, however, show an average shortening of 13 percent, in contrast to the 24-percent average increase of this axis in the study area.

The pattern of total strain in slate at the two localities that contain ellipsoidal spots are evaluated in a logarithmic deformation plot (fig. 27). Points A through N, from the Buffalo Hump Formation of the study area, are widely scattered on the plot; most points, however, fall into the field of flattening; and a few points (C–E) fall in the field of constriction. Points Q through S, from the Stensgar Dolomite near Chewelah, plot close to the line of plane strain at constant volume, although a 20-percent volume decrease has been assumed. Many ellipsoids are in the vicinity of the mean strain found in the Late Proterozoic Toby Conglomerate (correlative with the conglomerate member of the Huckleberry Formation; fig. 27; Ross and Barnes, 1975, fig. 8) in southeastern British Columbia.

If the ellipsoidal spots indicate that total maximum elongation in the slate averages no more than 200 percent, then either the 300- to 500-percent clast elongations in conglomerates must reflect primary clast shape, or the deformation path followed by the slate was complex, and the present ellipsoid shapes may not reflect the total mean strain; the strain increments of these clasts cannot be easily distinguished. During elastic recovery (Tobisch and Fiske, 1976, p. 1419) axes of ellipsoidal spots that were elongated during the previous deformational phase may have undergone an unknown, but probably small, amount of shortening along their long axes, while the clasts in the conglomerate may have been rigid enough to be unaffected. Under these circumstances, the clasts elongated more than 200 percent may more accurately reflect total elongation during the principal phases of compressional deformation if primary clast elongation can be ignored.

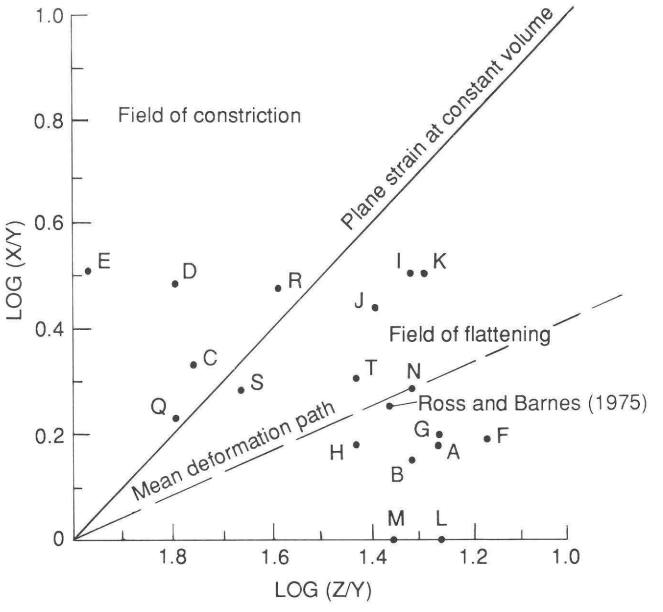

Figure 27. Logarithmic deformation plot.

Comparison of the ellipsoidal spots (fig. 27) illustrates the inhomogeneity of the deformation. The slate was flattened and constricted over a very wide range of strain values, although much of the strain appears to be characterized by flattening. Even the spots in a hand-specimen volume of slate of the Stensgar Dolomite show a wide scatter of strain values. The type of strain undergone in rocks of the study area, however, lies close to the mean deformation path followed in many other orogenic belts (Tobisch and others, 1977, p. 36–37), except that, in the study area, principal elongation parallels the trend of the orogen. Spots C, Q, R, and S lie closely along another, less common deformation path. The significance of such a variation in the type of strain within the magnesite belt is unknown.

Pinch-and-Swell Structure and Boudinage

Development of pinch-and-swell structure on a macroscopic scale in the Stensgar Mountain quadrangle resulted in rapid changes in the apparent stratigraphic thickness of mapped formations and members. Mesozoic faulting may account for some of the great variation in thicknesses of the Stensgar Dolomite, the McHale Slate, and quartzite of the Buffalo Hump Formation, as well as for stratigraphic duplication in the Deer Trail Group (Evans, 1987). However, thinning and thickening of the map units may also be due to the ductile phase of the Mesozoic deformation.

An example of mesoscopic pinch-and-swell structure occurs in a dolomite lens within slate of the McHale Slate in the SW¼ sec. 19, T. 31 N., R. 39 E. The longest and intermediate dimensions of this lens parallel cleavage in the slate. The sample (fig. 28) has quartz veins concentrated in the pinched zone, which has 57 percent of the thickness of the adjacent thicker part of the lens. Bedding laminae visible in thicker parts of the dolomite layer are obliterated in this pinched zone, which is linear and has an axis parallel to microcrenulations with amplitudes of 0.2 mm or smaller (L1) on cleavage of the adjacent slate (fig. 29). Other microcrenulations of about the same magnitude (L2) are perpendicular to the axis of the pinched zone. Other microcrenulations with slightly greater amplitudes (0.3 mm) (L3) trend at 50° to the smaller crenulations and are, in places, dominant (fig. 29). The larger crenulations (L3) and those perpendicular to the pinched zone (L2) probably predate the pinching because they are obliterated in parts of the necked zone. The smaller of these two sets of crenulations may be younger because it has preserved a possible kinematically significant angular relation to the pinched zone.

Quartz veins in the necked zone are of at least two kinds: (1) sets of veins intersecting at 70° (right side, fig. 28), and (2) veins at large angles to cleavage in the adjacent argillite and to the dolomite layer (left side, fig. 28). The veins end at the contact of dolomite and argillite. If the

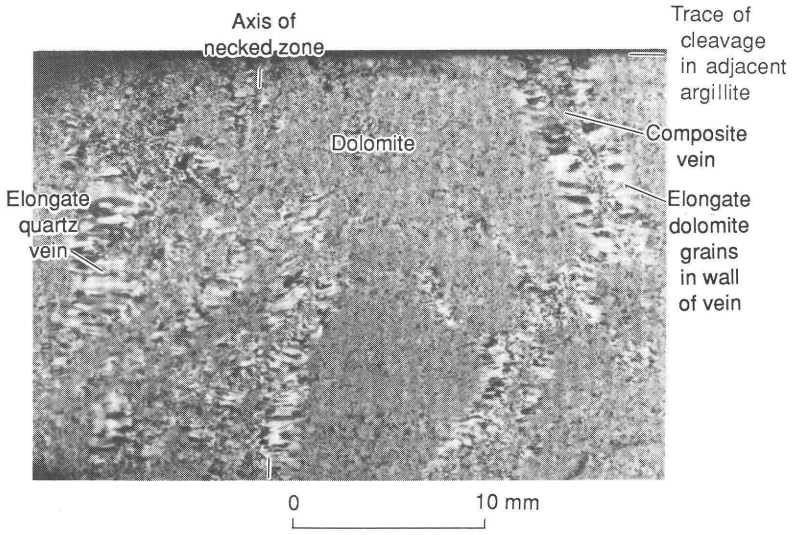

Figure 28. Necked region of dolomite lens in Buffalo Hump Formation. Fine-grained gray rock is dolomite; mottled white to black veins are mostly quartz and minor carbonate.

intersecting veins originated as conjugate fractures, stress axes may be determined from models of fracturing in which fault planes are related to the stress ellipsoid (Anderson, 1951; Durney, 1979; Casey, 1980). According to these models, the acute dihedral angle between the fracture sets encloses the maximum-principal-compressive-stress axis, σ_1, when a volume increase accompanies shearing; and the least-principal-compressive-stress axis, σ_3, is at right angles to it and the axis of intersection of fracture surfaces. In the necked zone of the dolomite, σ_1 would, by this criterion, be perpendicular to the lens and to cleavage, whereas σ_2 would be parallel to the intersection of fractures and at a low angle to the pinched zone, and σ_3 would be oriented at a high angle to this zone in the plane of cleavage.

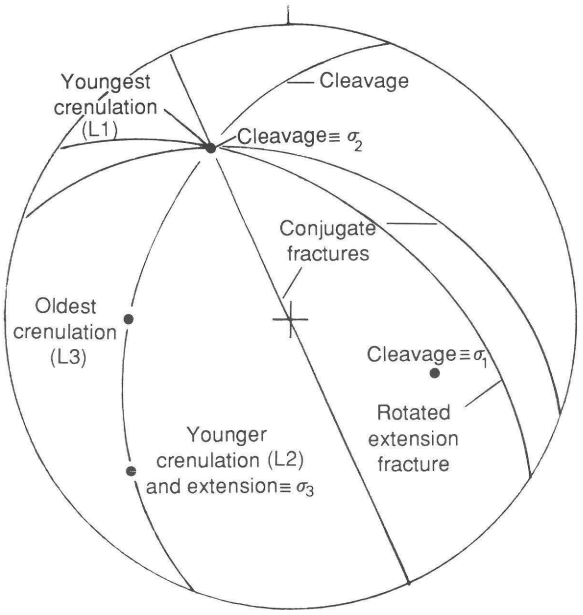

Figure 29. Orientation diagram of structural elements in sample shown in figure 28.

Using the terminology of Durney and Ramsay (1973, p. 72), the veins shown in figure 28 can be described as composite; that is, they consist of two or more minerals arranged in zones parallel to the vein walls. They contain a discontinuous central zone of carbonate flanked by fine-grained quartz, which grades to relatively coarse, elongate quartz grains over a very short distance. Zones of elongate dolomite grains along the vein walls in figure 28 shows the trace of the direction of maximum extension during vein formation. Directions of elongation of quartz grains in the cores of oblique veins (right side, fig. 28) are at large angles to the vein walls.

Directions of grain elongation in these veins, like the grain elongations in pressure shadows described above, mark the direction of least principal compressive stress and greatest extension. According to this criterion, the greatest extension during vein growth was approximately parallel to the dolomite layer and to cleavage in the adjacent argillite, and approximately perpendicular to one set of crenulations (L1) on the cleavage and parallel to another set (L2). These relations, which are consistent with slip on cleavage in a direction perpendicular to L1, indicate that these rocks have a subfabric approximating a B⊥B′ tectonite, although the perpendicular linear elements may not be entirely contemporaneous.

The minimum extension parallel to cleavage in the necked zone can be crudely estimated by measuring the ratio of carbonate to quartz across the neck, assuming no

replacement of carbonate by quartz or vice versa. This component of extension, which would have occurred only after fracturing and vein formation, would exclude the ductile component of necking or possible rehealed fracturing in the dolomite. The minimum elongation estimated in this way is 35 percent. Parts of the dolomite away from the neck would most likely have undergone substantially less elongation during this phase of deformation.

The long axis of the dolomite lens plunges 25°, S. 48° W., not far from the orientation of the oldest crenulations; this axis was probably established during an early phase of the deformation.

FABRIC DATA

Methods

Standard techniques of structural analyses were used (Turner and Weiss, 1963; Ramsay, 1967): gathering numerous attitudes of bedding, cleavages, veins, lineations, and fold axes, along with detailed observations of fold styles and of the geometric relations among fabric elements.

The Deer Trail Group is subdivided into the plates described above (fig. 3) and by Evans (1987). The structural elements in each plate were compiled separately, except that data from plate b and part of plate c were combined in the southwestern part of the study area; these plates are hereafter designated areas I through IV. Fabric data in these four areas were compared to detect any variations in the orientation or degree of development of fabric elements. Fabric data from the conglomerate member of the Huckleberry Formation, the Addy Quartzite, and the Old Dominion Limestone were also compiled and are discussed separately. Conglomerate of the Huckleberry Formation, the Addy Quartzite on Huckleberry and Lane Mountains, and the Old Dominion Limestone are designated areas V, VI, VII, and VIII, respectively (fig. 3).

Structural data were plotted as points on the lower hemispheres of equal-area projections. North is indicated by a short line pointing to the top of the page; vertical is indicated by the cross in the center of the primitive circle. Some structural data (n>25) were contoured on equal-area lower-hemisphere projections by the method originally described by Kamb (1959), wherein a variable counting area is used. The area is a function of the number of data points and the frequency of significant deviations from a uniform spatial distribution. Stereograms are contoured in intervals of 2σ and 4σ, where 2σ is the expected number of data points within a counting area for a uniform distribution across the entire stereogram. A point density greater than 3σ is considered to be a significant deviation from a random distribution. Pole-free areas indicate possibly significant absence of data points.

Deer Trail Group (Areas I–IV)

The fabric data from areas I through IV are shown on plate 1: contour and point diagrams for poles to bedding and cleavage and linear elements, and point diagrams of intersecting linear elements.

In the Deer Trail Group, bedding and S_1 cleavage, which parallels bedding, on average strike northeast and dip about 45° NW. Fabric diagrams 1 through 4 on plate 1 show the extent of variation in bedding attitudes. The greatest variation occurs in area I, which has a subordinate concentration of poles that represent beds dipping northeast. In areas I through III, poles to bedding lie along great circles that define beta axes plunging at moderate angles north and northwest.

Slaty cleavage, S_2, varies widely in orientation, but all four areas show a consistent average orientation that strikes north-northeast and dips steeply west (fabric diagrams 5–8, pl. 1). The frequency distribution of the angles between cleavage and bedding is shown in figure 30; angles range from 0° to 90°, with a mode in the range 30°–40°.

The axes of folds of bedding and cleavage, which are subparallel in each area, are included together in fabric diagrams 9 through 12 (pl. 1). The mean orientations of most folds plunge at low to moderate angles north-northwest and northwest. In areas I and II, the mean orientations of fold axes are very close to the beta axes (diagrams 9, 10, pl. 1). In area III, the beta axis and the mean of fold axes are 25° apart (diagram 11). In area IV, where a beta axis was not determined, the linear elements form two 6σ maxima (diagram 12), one of which plunges north-northwest, like the mean fold axes of areas I through III. The subordinate concentration of fold axes plunges steeply west but lies close to the dominant cleavage in the study area.

The axes of the macroscopic anticline and syncline in area I (fig. 3) are subparallel to the north-northwest-plunging minor-fold axes. This relation strongly suggests synchroneity of the large and minor folds (see subsection above entitled "Folds").

Point diagrams 13 through 16 (pl. 1) show intersecting crenulations and fold axes in areas I through IV. These linear elements suggest that two or more sets of folds developed in each of these areas, although some sets are not clearly defined on fabric diagrams 9 through 12. The poorly defined fold sets include steep folds plunging mostly west to southwest in areas I and II and northeast-plunging folds in areas II and III. In area IV, the intersecting folds clearly reflect the two fold-axis concentrations shown in diagram 12.

A subordinate cleavage, S_3, was identified at 19 localities in areas I through IV; it includes subordinate slaty cleavage, axial-plane cleavage, and fracture cleavage, steeply dipping to vertical and varying widely in strike (fig. 31*A*). Angles between the dominant and subordinate cleav-

ages range from 40° to 90°. Minor folds and crenulations of cleavage at 18 of these localities plunge at low to steep angles, mostly in the northwest quadrant (fig. 31*B*). Many folds associated with S_3 are oriented like the more steeply plunging fold group in area IV, and like the poorly defined, west-plunging fold groups in areas I and II. These relations suggest that the steeply plunging folds plotted in diagrams 12 through 14 could have been caused by folding at cleavage intersections, although subordinate cleavages were not identified at many localities at which these steeply plunging folds were observed.

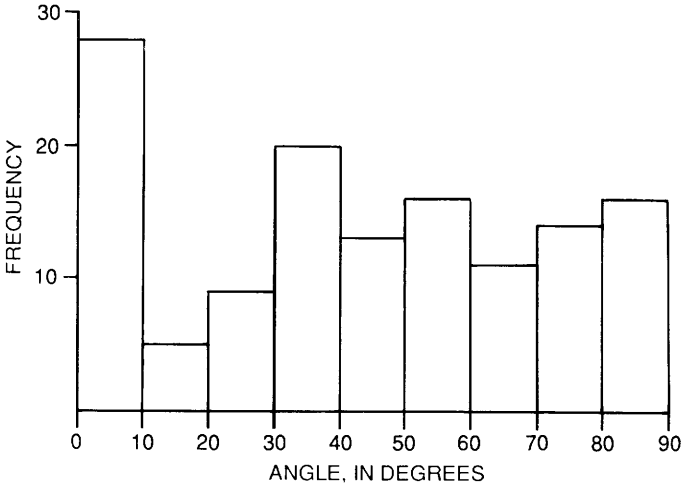

Figure 30. Angles between slaty cleavage and bedding in the Deer Trail Group at 137 localities in areas I through IV.

The subordinate cleavages clearly postdate the dominant slaty cleavage (fig. 12), at least in such rock types as argillite, because most of these subordinate cleavages would be unlikely to survive formation of the dominant cleavage, and they appear to cut across the slaty cleavage. Therefore the relatively poorly defined set of folds that plunge steeply west and are associated with the subordinate cleavage postdate the fold set plunging at low to moderate angles north-northwest.

No evidence was found to suggest a relation of the few northeast-plunging folds in areas II and III to other structural elements.

Area V

The conglomerate member of the Huckleberry Formation contains little bedding. Slaty cleavages in the unit have a mean orientation much like the means of cleavages in the Deer Trail Group, but over a smaller range of attitudes (diagram 17, pl. 1).

Crenulations on cleavages fall into two groups: (1) one group plunging at low angles north-northeast and south-southwest, and (2) another group plunging steeply (diagram 18). Both groups are about equally developed; they may correspond to the groups of linear elements in area IV. The average angle between intersecting crenulations at six localities is 82°, suggesting that these two groups of crenulations could be conjugate sets in a B⊥B′ tectonite.

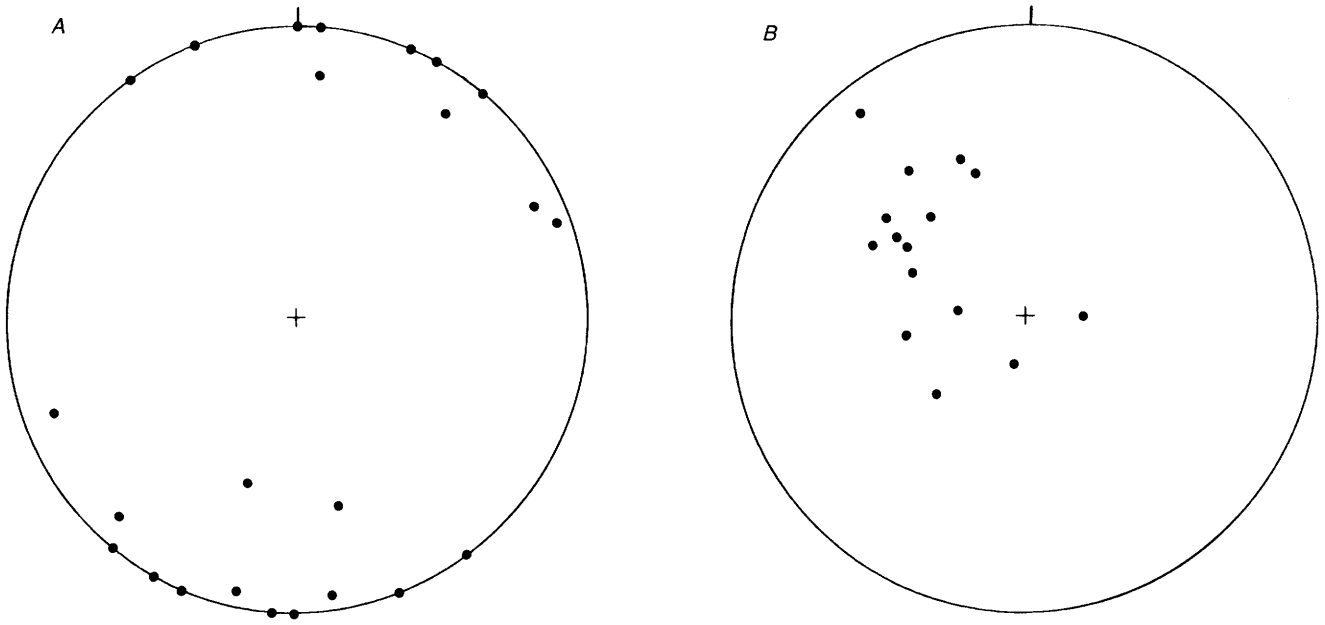

Figure 31. Orientation diagrams of subordinate cleavages and related folds in the Deer Trail Group in areas I through IV. *A*, Poles of subordinate cleavages. 24 points. *B*, Fold axes at intersections of subordinate cleavages and slaty cleavage or bedding. 15 points.

Area VI

Bedding in the Addy Quartzite on Huckleberry Mountain dips on average about 45° W-NW., close to the attitude of bedding in the Deer Trail Group (diagram 19, pl. 1). The similarity in bedding attitudes of the Proterozoic and Lower Cambrian rocks implies that much of the present orientation of bedding in the Proterozoic rocks is due to post-Early Cambrian tilting.

Cleavage is typically absent in the Addy Quartzite. At one locality, however, conspicuous fracture cleavage strikes N. 5° W. and dips 65° E.

Axes of minor folds (broad warps, crenulations of bedding) in area VI plunge at low to moderate angles north-northwest and northwest, like many of the linear elements in areas I through IV (diagram 20, pl. 1). At one locality, intersecting crenulations are 80° apart. The west-plunging crenulation may correlate with a subordinate set of folds found in areas I, II, and IV.

Area VII

Bedding in the Addy Quartzite on Lane Mountain dips about the same as in the quartzite on Huckleberry Mountain (diagram 21, pl. 1). Poles of bedding in area VII, however, appear to be distributed along a great circle that defines a beta axis plunging northwest. This relation strongly suggests that area VII, though in the footwall of the Lane Mountain thrust, was affected by the same deformation that affected the hanging wall. At one locality, two crenulations were found that intersect at 92° (diagram 22). One crenulation is close to the beta axis, and the other plunges southwest and may correlate with subordinate folds in areas I, II, and IV.

Area VIII

Bedding in the generally poorly exposed Old Dominion Limestone of area VIII dips steeply west. At one exposure, crenulations on bedding plunge 10°, N. 10° E., not far from the orientation of many minor-fold axes in the older rocks and close to that of some crenulations in areas V and VI. This evidence suggests that the Old Dominion Limestone was at least slightly affected by the same deformation that resulted in slaty cleavage and mostly minor folding in older rocks of the quadrangle.

Quartz Veins

Quartz veins in the Deer Trail Group and the Addy Quartzite (fig. 32) fall into two main groups. One group (A) approximately parallels bedding and cleavage but more closely parallels bedding; the other group (B) is at high angles to cleavage. Veins of group B may have originated as tension fractures parallel to the maximum-principal-compressive-strain axis associated with development of the principal cleavage, S_2. Veins of group A would be unlikely to form under the strain during which slaty cleavage developed because the planes now occupied by these veins would have been under compression, especially the veins parallel to cleavage. Therefore, these veins probably developed after the principal compression or during a phase of stress rebound when the principal compression was redirected at a low angle to cleavage and bedding (Tobisch and Fiske, 1976, p. 1419).

Extension Structures

Elongate clasts, pressure shadows, and extension directions deduced from pinch-and-swell structure point to a principal extension oriented subhorizontally and trending north-northwest to north-northeast (fig. 33). Although some clast elongations—for example, in the Monk Formation and at H3 in the Huckleberry Formation—parallel fold axes, others range from 5° to 32° to nearby fold axes, indicating that many of these two kinds of structural elements are not exactly parallel.

Synopsis

Synoptic diagrams of the principal planar and linear elements in the study area are shown in figure 34. Most bedding and the principal cleavage, S_2, are close together, separated by about 25° (fig. 34*A*). Bedding in area I is bimodal, with one group of beds close to 90° from the rest of bedding in the study area.

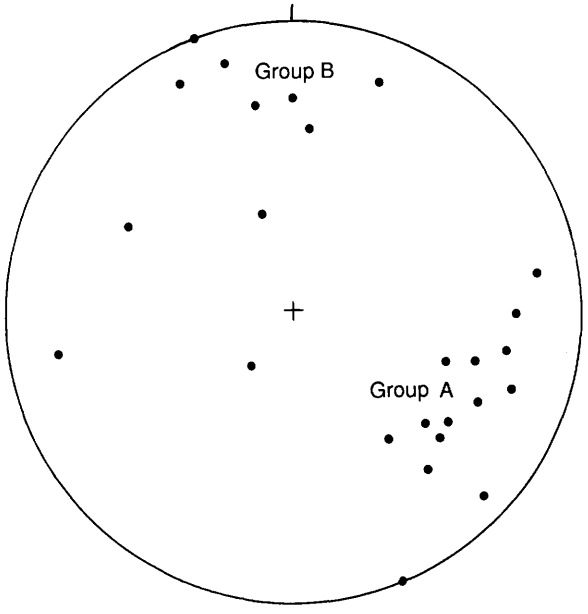

Figure 32. Orientation diagram of poles to quartz veins in the Deer Trail Group and the Addy Quartzite.

Linear elements, including macroscopic- and mesoscopic-fold axes in bedding, mesoscopic-fold axes in cleavage (including microcrenulations), and beta axes, which may also represent fold axes, fall into at least three main groups (figs. 34*B*–34*D*). (1) The best developed group plunges at low to moderate angles, mostly north to northwest (fig. 34*B*). (2) Elements of a second group, less well developed over the study area, plunge at moderate to steep angles, mostly in the southwest quadrant (fig. 34*C*). (3) Elements of a third group, very poorly developed in the study area, plunge at low angles northeast (fig. 34*D*). Group 1, the largest, which lies about the intersection of bedding and the principal cleavage, S_2, is probably related to formation of the cleavage. Group 2 coincides with folds known to be related to intersections of the principal cleavage and generally poorly developed younger cleavages, and so it is most likely the younger of these two fold groups. However, the possibility that groups 1 and 2 constitute a B⊥B′ tectonite cannot be ruled out. No information was found regarding the relation of group 3 elements to those of the other two groups.

Quartz veins at high angles to the dominant cleavage and pulled-apart clasts point to brittle extension in a direction close to the plane of slaty cleavage and at a small angle to fold axes of group 1. This direction of elongation corresponds closely to the general clast and nodule elongation and extension directions inferred from pressure shadows and pinch-and-swell structure.

The dynamothermal deformation affected the Proterozoic rocks most intensely. Evidence of strain is progressively more sparse upward in the section above the conglomerate member of the Huckleberry Formation. This apparent gradation in the intensity of deformation may be related to lithology because the argillaceous Proterozoic units are the most deformed, but it may also result from variation in strain across a duplex fault zone.

COMPARISON WITH FABRIC ELSEWHERE IN NORTHEASTERN WASHINGTON

The fabric described above for the Stensgar Mountain quadrangle resembles part of the fabric described by Thole and Mills (1979) for metasedimentary rocks of the magnesite belt southwest of Chewelah, including parts of the Stensgar Mountain quadrangle (fig. 1), in that it comprises both large- and small-amplitude folds plunging at generally low angles north-northeast, north, and north-northwest, with a steeply west dipping axial-plane foliation (cleavage) and secondary folds plunging steeply west at large angles to the earlier folds. They also noted pebble elongation in conglomerate of the Huckleberry Formation and the Addy Quartzite, pillow elongation in volcanic rocks of the Huckleberry Formation, and boudins in the Edna Dolomite subparallel to folds plunging north. Their study emphasized an analysis of joints in sedimentary rocks, including the Deer Trail Group, the Addy Quartzite, and the Covada Group (which occurs west of the Stensgar Mountain quadrangle). They distinguished seven sets of joints. Two sets, one dipping east at varying angles and striking north-south, the other dipping south at varying angles and striking northeast to northwest, are thought to be related to principal folding during the Mesozoic. One of these two sets approximately parallels, and the other is at right angles to, the principal group of fold axes. Many quartz veins in the Stensgar Mountain quadrangle have attitudes like those of these two sets (fig. 32). A third set of joints, striking on average N. 78° E. and dipping 80° SE., was believed by Thole and Mills to postdate the first two sets, but it is absent in Cretaceous granitic rocks nearby, and so it is considered to predate these intrusions. The other four sets are developed in relation to emplacement of granitic rocks and subsequent emplacement of dikes and veins in the plutons.

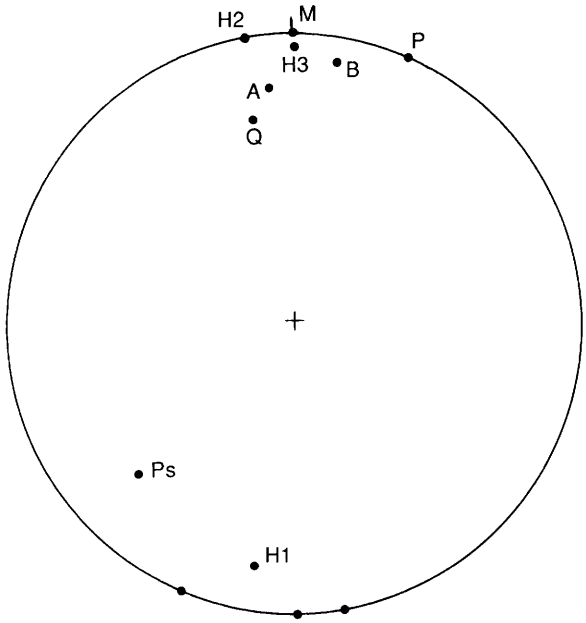

Figure 33. Orientation diagram of extension structures. A, elongation of clasts in Addy Quartzite in SE¼ sec. 22, T. 31 N., R. 38 E.; B, elongation of clasts in Buffalo Hump Formation in NE¼ sec. 3, T. 30 N., R. 38 E.; H1, elongation of quartzite and siltite clasts in Huckleberry Formation in SW¼ sec. 29, T. 32 N., R. 39 E.; H2, brittle elongation of quartz clast in Huckleberry Formation in SE¼ sec. 34, T. 31 N., R. 38 E.; H3, elongation of shale clasts in Huckleberry Formation in SE¼ sec. 12, T. 31 N., R. 38 E.; M, elongation of clasts in Monk Formation in NW¼ sec. 15, T. 31 N., R. 39 E.; P, elongation of pressure shadows in McHale Slate in SW¼ sec. 19, T. 31 N., R. 39 E.; Ps, elongation inferred from pinch-and-swell structure in McHale Slate in SW¼ sec. 29, T. 31 N., R. 39 E.; Q, pole of mean attitude of group B quartz veins.

The fabric of the rocks in the Stensgar Mountain quadrangle is generally consistent with that of other deformed metasedimentary rocks elsewhere in northeastern Washington (Mills and Nordstrom, 1979), and with the regional structural synthesis of the Mesozoic deformation of the Kootenay arc in Washington (Snook and others, 1982; Ellis, 1986; Ellis and Watkinson, 1987; and Watkinson and Ellis, 1987). According to these studies, the metasedimentary rocks of the region were subjected to greenschist-facies dynamothermal metamorphism during the Jurassic(?). Early, generally north-south-trending folds with axial-plane cleavage developed at that time. Maximum elongation paralleled early-fold axes, which were refolded coaxially. Although the Stensgar Mountain quadrangle also has a major subfabric with components like those described by Mills and Nordstrom (1973), Snook and others (1982), Ellis (1986), Ellis and Watkinson (1987), and Watkinson and Ellis (1987), rocks in the present study area lack obvious

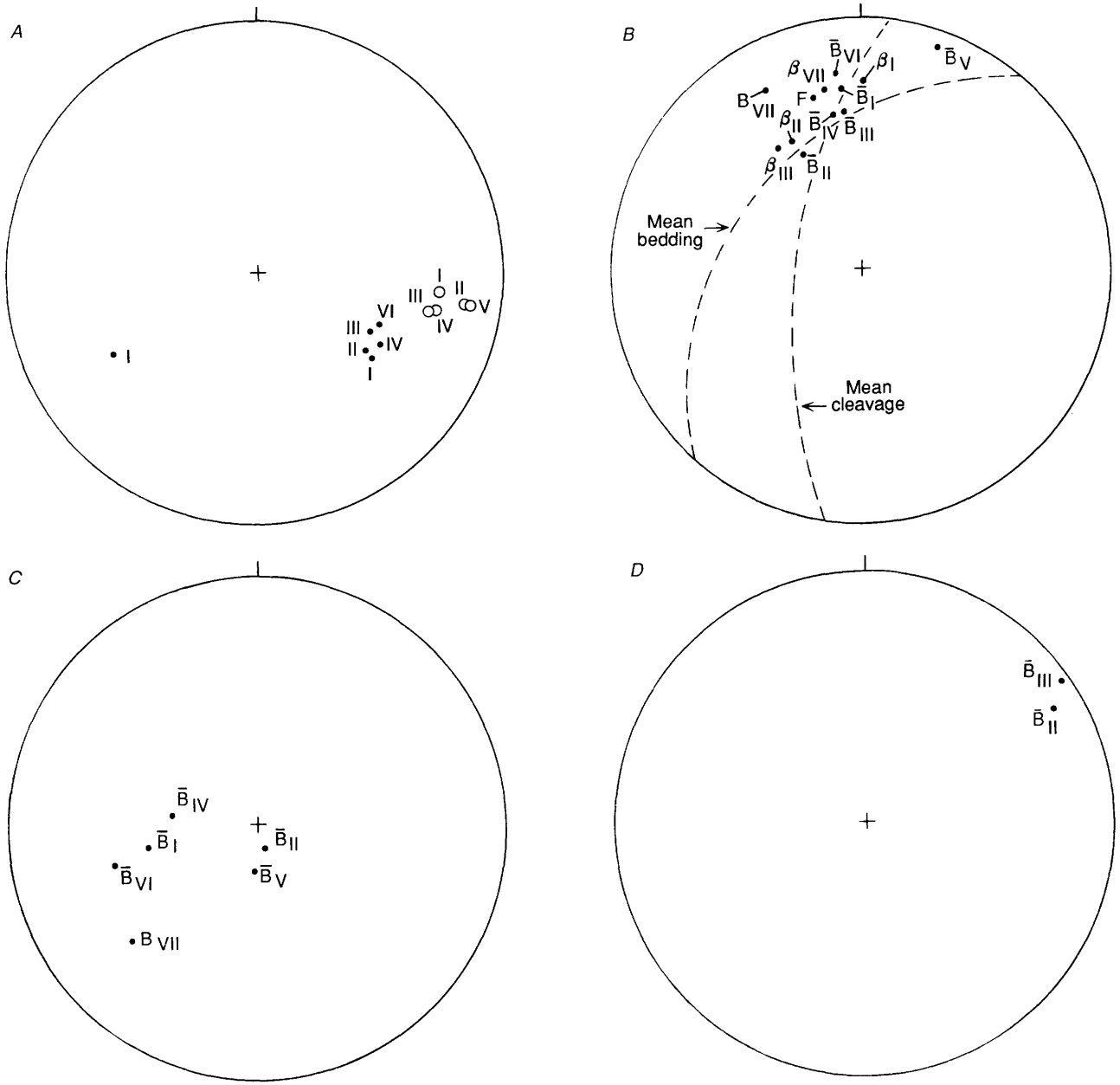

Figure 34. Synoptic diagrams of principal planar and linear elements in the study area. *A*, Bedding (dots) and slaty cleavage (circles). *B–D*, Linear elements in groups 1 through 3. Dashed great circle, mean attitudes of bedding and slaty cleavage in the study area. B, individual fold axis; $\bar{B}$, mean of fold axes; F, large folds in the Togo Formation; β, beta axis. Roman numerals refer to structural areas described in text.

multiple coaxial refolding of early folds (Thole and Mills, 1979) and generally are not so intensely deformed as some of the rocks farther north (see Mills and Nordstrom, 1973, figs. 4–15).

The stratigraphic similarities between units of the Deer Trail Group and possibly correlative units of the Belt Supergroup in the Chewelah-Loon Lake area were described by Evans (1987). The rock units of these two Proterozoic assemblages also have structural similarities as well as differences. Geologic interpretations of the Chewelah-Loon Lake area by Miller and Clark (1975, pl. 1, cross secs. *A–A'*, *B–B'*) show large deformed thrusts and at least one major recumbent isoclinal fold in the Belt Supergroup. In addition, these rocks have a subfabric that includes components similar to the fabric of the Deer Trail Group: (1) The beta axis defined by poles of bedding plunges 10°, S. 3° W., in the Loon Lake area and is subhorizontal and trends N. 17° E. in the Chewelah area; (2) locally developed cleavage and schistosity are complex but include an important subset, planes of which dip steeply or are vertically and strike north to north-northeast, like cleavage in the Stensgar Mountain quadrangle; and (3) most minor folds in the Chewelah area plunge at low angles north and south-southwest. In contrast, most minor folds in the Loon Lake area plunge east. Although the total strain in the Belt Supergroup just east of the magnesite belt may differ from that in the Deer Trail Group, a subfabric in Belt strata in the Chewelah-Loon Lake area is similar to the dominant mesoscopic fabric of the Deer Trail Group—another similarity between these two rock assemblages.

STRUCTURAL DEVELOPMENT

The Proterozoic section was tilted slightly before the Lower Cambrian Addy Quartzite was deposited, as is probably reflected in the angular unconformity at the base of the Addy Quartzite and the 8° difference in the average dip of beds in the Deer Trail Group and Addy Quartzite. Miller and Clark (1975, p. 27) mentioned that the Proterozoic rocks below the Addy Quartzite were faulted and broadly folded before the Addy was deposited. The absence of the Monk Formation in the Windermere section of Huckleberry Mountain may have resulted in part from uplift and erosion due to this Late Proterozoic faulting and folding.

Beds in the section of the Proterozoic and Lower Cambrian rocks were rotated toward slaty cleavage during the Mesozoic dynamothermal metamorphism described in this report. The amount of rotation can be estimated by using the graphical method of Ramsay (1967, p. 129-132). Assuming strains like the ones for spot A in table 1 and a present average bedding striking N. 30° E. and dipping 46° NW., the bedding was rotated 12° during the Mesozoic deformation. Therefore, the sedimentary rocks must have undergone substantial tilting before the dynamothermal metamorphism because the average pretectonic bedding had a strike of N. 46° E. and a dip of 42° NW.

Both the duplex thrusting and the dynamothermal metamorphism are pre-Late Jurassic and possibly Early Jurassic or Triassic, on the basis of the ages of posttectonic plutons in the region (see section above entitled "Geology"). The timing of faulting and dynamothermal metamorphism, however, is not entirely clear. The matrix of cataclasite found along the hanging wall of the Lane Mountain thrust (Evans, 1987) contains unbrecciated porphyroblasts of minerals indicating greenschist-facies metamorphism. This rock suggests that the Lane Mountain thrust and, possibly, the duplex fault zone were active before, as well as after, the dynamothermal metamorphism. The substantial tilting of the section could have occurred during the initial faulting. Although the principal mesoscopic-fabric elements in the thrust plates within the duplex fault zone are nearly identical in types and orientations, faults within the duplex fault zone appear to be unaffected by the folding—a feature indicating that penetrative deformation occurred before the final movements within the duplex fault zone and that the final faulting involved little rotation.

Orientations of axes of the mean stress ellipsoid for formation of the slaty cleavage, S_2, can be generally inferred. During penetrative deformation, the principal compressive strain was perpendicular to slaty cleavage; principal elongation was in the plane of cleavage, probably subparallel to clast elongations. The intermediate strain was in the plane of cleavage and perpendicular to clast elongation. Stress axes during the deformation may have coincided with strain axes if the strains during this event greatly exceeded preexisting noncoaxial strains and if no significant mechanical anisotropies existed in the rock. In rocks of the Stensgar Mountain quadrangle, the greatest amount of penetrative strain most likely occurred during the Mesozoic deformation. Strain occurred during depositional loading because the Deer Trail Group was overlain by at least 2.5 km of the Windermere Group and at least 6 km of combined Late Proterozoic and Lower Cambrian rocks by the end of the Cambrian, and probably by a much greater thickness of overburden if the rest of the Paleozoic section of the region is included. Early compaction of argillaceous rock units of possibly as much as 50 percent is included in the approximately 67 percent estimated average shortening perpendicular to slaty cleavage during the Mesozoic, and is not a readily separable strain increment. Dimensional fabrics of the clasts and pressure shadows suggest that the mean stress axes during penetrative deformation had the following orientations: σ_1, the principal-compressive-stress axis, plunged at a low angle east-southeast, at a large angle to the mean attitude of slaty cleavage, S_2; σ_2, the intermediate-principal-compressive-stress axis, plunged steeply west-northwest; and σ_3, the minimum-prin-

cipal-compressive-stress axis, was subhorizontal and trended north-northeast, parallel to the principal elongations of clasts and the long axes of ellipsoids and pressure shadows.

The stress ellipsoid implied by the Lane Mountain and Stensgar Mountain thrusts—the floor and roof thrusts, respectively, of the duplex fault zone—may not be determinable from the fault models cited above. These models predict that, in the case of compressional stress, the acute dihedral angle between conjugate-slip surfaces encloses σ_1 and that σ_2 parallels the axis of intersection of the slip surfaces. The thrusts, however, lack conjugate-slip surfaces and appear to have many secondary faults (thrusts and connecting splays between the roof and floor thrusts). Therefore, it is unclear how the stress ellipsoid for the duplex fault zone can be evaluated in the absence of such additional information as slip direction. A stress-strain model for a duplex fault system is needed.

Stratigraphic separations suggest a large dip-slip component on the Lane Mountain thrust but a much smaller dip-slip component on the Stensgar Mountain thrust. Significant strike-slip components cannot be ruled out. If the fault models could be used for these faults, the mean σ_1 would be approximately subhorizontal and trend east-west, at least for the Lane Mountain thrust, assuming a large dip component of slip. The orientations of σ_2 and σ_3 during thrusting would have been the reverse of those during the penetrative deformation. Similarities in the orientations of σ_1 for thrusting and penetrative deformation may be fortuitous or could suggest a relation between these two events; they may have occurred during a long, multistage tectonic episode.

If the duplex thrusting and penetrative deformation were partly contemporaneous, the mean slip direction along the duplex fault zone may be reflected by strains within the duplex and in the surrounding rocks. If the duplex fault zone, consisting of deformed rocks of the Deer Trail Group, underwent north-northeast-trending extension during dynamothermal metamorphism, while the relatively undeformed Addy Quartzite in the footwall underwent little or no extension, lateral slip might be expected along the Lane Mountain thrust; however, no evidence was found to suggest a sense of slip. Slip along the Stensgar Mountain thrust is difficult to evaluate because no clear stratigraphic separation is evident across the thrust, and the basal conglomerate member of the Huckleberry Formation in the hanging wall is deformed like the Deer Trail Group in the footwall. In the Addy quadrangle, the possible extension of the Stensgar Mountain thrust has a much more obvious stratigraphic separation (Miller and Yates, 1976), but this information provides no clue regarding the magnitude of the strike component of slip. Inasmuch as the conglomerate member of the Huckleberry Formation underwent the same kind of pervasive deformation, involving extension along the strike of the orogen, as the Deer Trail Group, whereas the volcanic rocks member did not, lateral slip between the conglomerate member and the mostly undeformed volcanic rocks member may have occurred.

Although all the sedimentary rocks in the Stensgar Mountain quadrangle were affected by the Mesozoic deformation, the Deer Trail Group seems to be the most dismembered. The Deer Trail Group may have undergone intense dismemberment because of the large volume of incompetent argillaceous metasedimentary rocks in the section: Two-thirds of the stratigraphic thickness of the Deer Trail Group is slate and minor siltite. The bulk competence of the Deer Trail Group was probably very low in comparison with that of other units, such as the Addy Quartzite and the volcanic rocks member of the Huckleberry Formation. In a sense, the Deer Trail Group and, possibly, the intensely deformed basal conglomerate member of the Huckleberry Formation behaved as broad zones of shearing.

Although the dynamothermal metamorphism is treated as a single, though complex, event, the structures attributed to it could actually be the cumulative effects of several nearly coaxial episodes of deformation (Tobisch and Fiske, 1982). The discussion above suggests a succession of events seemingly closely clustered about development of the slaty cleavage. The dynamothermal deformation, though dated at pre-Late Jurassic, could have consisted of several separate pulses occurring sporadically over tens of millions of years. The elastic recovery postulated by Tobisch and Fiske (1976, p. 1419) and possibly affecting at least the microfabric of the rocks of the study area could have occurred after each tectonic pulse.

If the direction of maximum elongation is correctly shown by clast elongation and the other extension indicators, it plunges at a low angle north-northeast, approximately parallel to the trend of the Kootenay arc. According to Snook and others (1982), Ellis (1986), Ellis and Watkinson (1987) and Watkinson and Ellis (1987), this principal extension direction is typical for the arc in northeastern Washington; it is not, however, typical for deformation belts in general (Wood, 1973; Tobisch and others, 1977, p. 37). Extension parallel to an orogenic belt would be expected to be inhibited, whereas upward extension would require less energy. However, the seemingly more plausible upward principal extension does not appear to have occurred in the Kootenay arc of northeastern Washington until later in the deformation (Watkinson and Ellis, 1987). Ellis (1986), Ellis and Watkinson (1987), and Watkinson and Ellis (1987) explain the extension subparallel to the Kootenay arc as a result of early folding in the footwall of an obliquely subducting continent. The early deformation in the footwall reflects oblique subduction, but the orientation of the axis of principal extension will always be closer to the trend of the orogen than the direction of oblique convergence.

SUMMARY

1. Except for probable minor Late Proterozoic tilting, the sedimentary rocks of the Stensgar Mountain quadrangle do not appear to have been much deformed until the Mesozoic.
2. The entire Deer Trail Group comprises a duplex fault zone that has the Lane Mountain thrust as the floor thrust and the Stensgar Mountain thrust as the roof thrust. This duplex fault zone, which is the principal structure in the study area, most likely formed during the Jurassic or Triassic.
3. The Mesozoic deformation was complex and involved at least three stages: (1) thrusting, (2) penetrative dynamothermal metamorphism, and (3) renewed thrusting. Initial thrusting may have included formation of the duplex fault zone, moderate tilting of the sedimentary and volcanic rocks, and, possibly, low-grade thermal metamorphism. The dynamothermal metamorphism could have been accompanied by continued slip on faults, especially the floor and roof thrusts of the duplex fault zone. Later thrusting involved the floor and roof thrusts and connecting splays, which appear to be unaffected by the penetrative deformation.
4. The principal fabric elements of the penetrative deformation are slaty cleavage, dipping steeply west, in the Deer Trail Group and the basal conglomerate member of the Huckleberry Formation, and minor folds, plunging at low to moderate angles north-northwest and north, in all units except the volcanic rocks member of the Huckleberry Formation. The slaty cleavage implies a mean-principal-shortening direction plunging at a low angle east-southeast. Elongations of clasts and pressure shadows point to a subhorizontal mean-principal-extension axis trending north-northwest to north-northeast, at a small angle to most fold axes. Deformation was generally inhomogeneous and characterized by flattening in the study area.
5. The penetrative deformation in the Stensgar Mountain quadrangle also affected the rest of the magnesite belt and is related to a regional deformation in other parts of northeastern Washington and in southeastern British Columbia that may be a result of oblique convergence during Mesozoic subduction. Subfabrics in the Belt Supergroup of the nearby Chewelah-Loon Lake area resemble the dominant subfabric of the Deer Trail Group but are not so well developed as those in the study area. The rocks in some parts of northern Washington were even more highly deformed during Mesozoic penetrative deformation than those in the study area.
6. The Mesozoic penetrative deformation may have consisted of several compressional pulses, more or less coaxial, with intervening periods of elastic rebound.

REFERENCES CITED

Aalto, K.R., 1971, Glacial marine sedimentation and stratigraphy of the Toby conglomerate (upper Proterozoic), southeastern British Columbia, northwestern Idaho and northeastern Washington: Canadian Journal of Earth Sciences, v. 8, no. 7, p. 753–787.

Anderson, E.M., 1951, Dynamics of faulting and dyke formation with applications to Britain (2d ed.): Edinburgh, Oliver and Boyd, 206 p.

Avé Lallemant, H.G., 1977, Structural evolution of the northern part of the Melones fault zone and adjacent areas in California: Geological Society of America Abstracts with Programs, v. 11, no. 3, p. 67.

Beutner, E.C., 1978, Slaty cleavage and related strain in Martinsburg Slate, Delaware Water Gap, New Jersey: American Journal of Science, v. 278, no. 1, p. 1–23.

Bennett, W.A.G., 1941, Preliminary report on magnesite deposits of Stevens County, Washington: Washington Division of Geology Report of Investigations 5, 25 p.

Borradaile, G.J., Bayly, M.B., and Powell, C.M., eds., 1982, Atlas of deformational and metamorphic rock fabrics: New York, Springer-Verlag, 551 p.

Boyer, S.E., and Elliott, David, 1982, Thrust systems: American Association of Petroleum Geologists, v. 66, no. 9, p. 1196–1230.

Byrne, Tim, 1984, Early deformation in melange terranes of the Ghost Rocks Formation, Kodiak Islands, Alaska: Geological Society of America Special Paper 198, p. 21–51.

Campbell, Ian, and Loofbourow, J.S., Jr., 1962, Geology of the magnesite belt of Stevens County, Washington: U.S. Geological Survey Bulletin 1142-F, p. F1–F53.

Casey, M., 1980, Mechanics of shear zones in isotropic dilatent materials: Journal of Structural Geology, v. 2, p. 143–147.

Cloos, Ernst, 1947, Oölite deformation in the South Mountain fold, Maryland: Geological Society of America Bulletin, v. 58, no. 9, p. 843–917.

——— 1971, Microtectonics along the western edge of the Blue Ridge, Maryland and Virginia: Baltimore, Johns Hopkins University Press, 234 p.

Dalrymple, G.B., 1979, Critical tables for conversion of K-Ar ages from old to new constants: Geology, v. 7, no. 11, p. 558–560.

Dieterich, J.H., 1969, Origin of cleavage in folded rocks: American Journal of Science, v. 267, no. 2, p. 155–165.

——— 1970, Computer experiments on mechanics of finite amplitude folds: Canadian Journal of Earth Sciences, v. 7, no. 2, pt. 1, p. 467–476.

Dieterich, J.H., and Carter, N.L., 1969, Stress-history of folding: American Journal of Science, v. 267, no. 2, p. 129-154.

Durney, D.W., 1979, Dilation in shear zones and its influence on the development of en-echelon fractures [abs.]: Shear Zone Conference, Barcelona, p. 30–31.

Durney, D.W. and Ramsay, J.G., 1973, Incremental strains measured by syntectonic crystal growth, *in* DeJong, K.A., and Scholten, Robert, eds., Gravity and tectonics: New York, John Wiley & Sons, p. 67–96.

Ellis, M.A., 1986, Structural morphology and associated strain in the central Cordillera (British Columbia and Washington):

Evidence of oblique tectonics: Geology, v. 14, no. 8, p. 647–650.

Ellis, M.A., and Watkinson, A.J., 1987, Orogen-parallel extension and oblique tectonics: The relation between stretching lineations and relative plate motions: Geology, v. 15, no. 11, p. 1022–1026.

Evans, J.G., 1987, Geology of the Stensgar Mountain quadrangle, Stevens County, Washington: U.S. Geological Survey Bulletin 1679, 23 p.

Fox, K.F., Jr., Rinehart, C.D., and Engels, J.C., 1977, Plutonism and orogeny in north-central Washington—timing and regional context: U.S. Geological Survey Professional Paper 989, 27 p.

Fyles, J.T., 1962, Two phases of deformation in the Kootenay arc: Western Miner and Oil Review, v. 35, no. 7, p. 20–26.

Gray, D.R., 1978, Cleavages in deformed psammitic rocks from southeastern Australia: Their nature and origin: Geological Society of America Bulletin, v. 89, no. 4, p. 577–590.

Groshong, R.H., Jr., 1975, "Slip" cleavage caused by pressure solution in a buckle fold: Geology, v. 3, no. 7, p. 411–413.

Groshong, R.H., 1976, Strain and pressure solution in the Martinsburg slate, Delaware Water Gap, New Jersey: American Journal of Science, v. 276, no. 9, p. 1131–1146.

Hedley, M.S., 1955, Lead-zinc deposits of the Kootenay arc: Western Miner, v. 28, no. 7, p. 31–35.

Hobbs, B.E., Means, W.D. and Williams, P.F., 1976, An outline of structural geology: New York, John Wiley and Sons, 571 p.

Kamb, W.B., 1959, Ice petrofabric observations from Blue Glacier, Washington, in relation to theory and experiment: Journal of Geophysical Research, v. 64, no. 11, p. 1891–1909.

Kerrich, Robert, and Allison, Ian, 1983, Flow mechanisms in rocks: Geoscience Canada, v. 5, no. 3, p. 109–118.

Miller, F.K., and Clark, L.D., 1975, Geology of the Chewelah-Loon Lake area, Stevens and Spokane Counties, Washington: U.S. Geological Survey Professional Paper 806, 74 p.

Miller, F.K., and Engels, J.C., 1975, Distribution and trends of discordant ages of the plutonic rocks of northeastern Washington and northern Idaho: Geological Society of America, v. 86, no. 4, p. 517–528.

Miller, F.K., and Yates, R.G., 1976, Geologic map of the west half of the Sandpoint 1°×2° quadrangle, Washington: U.S. Geological Survey Open-File Report 76-327, scale 1:125,000, 2 sheets.

Mills, J.W., and Nordstrom, H.E., 1979, Multiple deformation of Cambrian rocks in the Kootenay Arc, near Northport, Stevens County, Washington: Northwest Science, v. 47, no. 3, p. 185–202.

Oertel, Gerhard, 1971, Deformation of a slaty, lapillar tuff in the English Lake District: Reply: Geological Society of America Bulletin, v. 83, no. 2, p. 549–550.

Palmer, A.R., 1983, The Decade of North American Geology 1984 geologic time scale: Geology, v. 11, no. 9, p. 503–504.

Patterson, M.S., and Weiss, L.E., 1966, Experimental deformation and folding in phyllite: Geological Society of America Bulletin, v. 77, no. 4, p. 343–374.

Ramsay, J.G., 1967, Folding and fracturing of rocks: New York, McGraw-Hill, 568 p.

——— 1981, Tectonics of the Helvetic nappes, *in* McClay, K.R., and Price, N.J., eds., Thrust and nappe tectonics: Geological Society of London Special Publication 9, p. 197–210.

Ramsay, J.G., and Wood, D.S., 1973, The geometric effects of volume change during deformation processes: Tectonophysics, v. 16, no. 3–4, p. 263–277.

Rinehard, C.D., and Fox, K.F., Jr., 1972, Geology and mineral deposits of the Loomis quadrangle, Okanogan County, Washington: Washington Division of Mines and Geology Bulletin 64, 124 p.

Ross, J.V. and Barnes, W.C., 1975, Development of cleavages within diamictites of southeastern British Columbia: Canadian Journal of Earth Sciences, v. 12, no. 8, p. 1291–1306.

Rutter, E.H., 1976, The kinetics of rock deformation by pressure solution: Royal Society of London Philosophical Transactions, ser. A, v. 283, p. 203–217.

Siddans, A.W.B., 1972, Slaty cleavage—a review of research since 1815: Earth Science Reviews, v. 8, p. 205–232.

Snook, J.R., Ellis, M.A., Mills, J.W., and Watkinson, A.J., 1982, The Kootenay Arc in Northeast Washington [abs.]: Geological Society of America Abstracts with Programs, v. 14, no. 4, p. 235.

Thole, R.H., and Mills, J.W., 1979, Joint analysis of the magnesite belt of Stevens County, Washington: Northwest Science, v. 53, no. 2, p. 141–156.

Tobisch, O.T., and Fiske, R. S., 1976, Significance of conjugate folds and crenulations in the central Sierra Nevada, California: Geological Society of America Bulletin, v. 87, no. 10, p. 1411–1420.

——— 1982, Repeated parallel deformation in part of the eastern Sierra Nevada, California and its implications for dating structural events: Journal of Structural Geology, v. 4, no. 2, p. 177–195.

Tobisch, O.T., Fiske, R.S., Sacks, Steven, and Taniguchi, Dennis, 1977, Strain in metamorphosed volcaniclastic rocks and its bearing on the evolution of orogenic belts: Geological Society of America Bulletin, v. 88, no. 1, p. 23–40.

Turner, F.J., and Weiss, L.E., 1963, Structural analysis of metamorphic tectonites: New York, McGraw-Hill, 545 p.

Watkinson, A.J., and Ellis, M.A., 1987, Recent structural analyses of the Kootenay arc in northeastern Washington, *in* Schuster, J.E., ed., Selected papers on the geology of Washington: Washington Division of Geology and Earth Resources Bulletin 77, p. 41–53.

Weaver, C.E., 1920, The mineral resources of Stevens County: Washington Geological Survey Bulletin 20, 350 p.

Weyl, P.K., 1959, Pressure solution and the force of crystallization—a phenomenological theory: Journal of Geophysical Research, v. 62, p. 2001–2025

White, W.H., 1959, Cordilleran tectonics in British Columbia: American Association of Petroleum Geologists Bulletin, v. 43, no. 1, p. 60–100.

Whitten, E.M.T., 1966, Structural geology of folded rocks: Chicago, Rand McNalley and Co., 678 p.

Williams, P.F., 1972, Development of metamorphic layering and cleavage in low grade metamorphic rocks at Bermagui, Australia: American Journal of Science, v. 272, no. 1, p. 1–47.

Williams, P.F., 1976, Relationships between axial-plane foliations and strain: Tectonophysics, v. 30, no. 3–4, p. 181–196.

Wood, D.S., 1973, Patterns and magnitudes of natural strain in

rocks: Royal Society of London Philosophical Transactions, ser. A, v. 27, no. 1239, p 373–382.

——— 1974, Current views of the development of slaty cleavage: Annual Review of Earth and Planetary Science, v. 2, p. 369–401.

Wood, D.S. and Oertel, Gerhard, 1980, Deformation in the Cambrian Slate belt of Wales: Journal of Geology, v. 88, no. 3, p. 285–308.

Wright, T.O., and Platt, L.B., 1982, Pressure dissolution and cleavage in the Martinsburg Shale: American Journal of Science, v. 282, no. 2, p. 122–135.

Yates, R.G., 1970, Geologic background of the Metaline and Northport mining districts, Washington, *in* Weissenborn, A.E., ed., Lead-zinc deposits in the Kootenay Arc: Washington Division of Mines and Geology Bulletin 61, p. 21–39.

Yates, R.G., Becraft, G.E., Campbell, A.B., and Pearson, R.C., 1966: Tectonic framework of northeastern Washington, northern Idaho, and northwestern Montana, *in* A symposium on the tectonic history and mineral deposits of the western Cordillera in British Columbia and neighboring parts of the United States: Canadian Institute of Mining and Metallurgy Special Volume 8, p. 47–59.

GPO 585-045/9758